Comprehensive multiphase chlorine chemistry in the box model CAABA/MECCA: Implications to atmospheric oxidative capacity

Meghna Soni[1, 2], Rolf Sander[3], Lokesh K Sahu[1], Domenico Taraborrelli[4], Pengfei Liu[5], Ankit Patel[6], Imran A Girach[7], Andrea Pozzer[3, 8], Sachin S Gunthe[6, 9], and Narendra Ojha[1]

[1]Physical Research Laboratory, Ahmedabad, India
[2]Indian Institute of Technology, Gandhinagar, India
[3]Atmospheric Chemistry Department, Max Planck Institute for Chemistry, Mainz, Germany
[4]Institute of Energy and Climate Research, Troposphere (IEK-8), Forschungszentrum Jülich GmbH, Jülich, Germany
[5]School of Earth and Atmospheric Sciences, Georgia Institute of Technology, Atlanta, GA, USA
[6]EWRE Division, Department of Civil Engineering, Indian Institute of Technology Madras, Chennai, India
[7]Space Applications Centre, Indian Space Research Organisation, Ahmedabad, India
[8]Climate and Atmosphere Research Center, The Cyprus Institute, Nicosia, Cyprus
[9]Centre for Atmospheric and Climate Sciences, Indian Institute of Technology Madras, Chennai, India

Correspondence: Meghna Soni (soni.meghna95@gmail.com) and Rolf Sander (rolf.sander@mpic.de)

Abstract. Tropospheric chlorine chemistry can strongly impact the atmospheric oxidation capacity and composition, especially in urban environments. To account for these reactions, the gas- and aqueous-phase Cl chemistry of the community atmospheric chemistry box model CAABA/MECCA has been extended. In particular, an explicit mechanism for $ClNO_2$ formation following N_2O_5 uptake to aerosols has been developed. The updated model has been applied to two urban environments with different concentrations of NO_x ($NO + NO_2$): New Delhi (India) and Leicester (United Kingdom). The model shows a sharp build-up of Cl at sunrise through Cl_2 photolysis in both the urban environments. Besides Cl_2 photolysis, $ClO+NO$ reaction, and photolysis of $ClNO_2$ and $ClONO$ are also prominent sources of Cl in Leicester. High-NO_x conditions in Delhi tend to suppress the night-time build-up of N_2O_5 due to titration of O_3 and thus lead to lower $ClNO_2$, in contrast to Leicester. Major loss of $ClNO_2$ is through its uptake on chloride, producing Cl_2, which consequently leads to the formation of Cl through photolysis. The reactivities of Cl and OH are much higher in Delhi, however, the Cl/OH reactivity ratio is up to ≈ 9 times greater in Leicester. The contribution of Cl to the atmospheric oxidation capacity is significant and even exceeds (by ≈ 2.9 times) that of OH during the morning hours in Leicester. Sensitivity simulations suggest that the additional consumption of VOCs due to active gas- and aqueous-phase chlorine chemistry enhances OH, HO_2, and RO_2 near the sunrise. The simulation results of the updated model have important implications for future studies on atmospheric chemistry and urban air quality.

1 Introduction

Chlorine (Cl) radicals are one of the most important players in the tropospheric chemistry (Seinfeld and Pandis, 2016; Ravishankara, 2009). Cl impacts the oxidative capacity of the atmosphere, radical cycling, and, therefore, can significantly alter the atmospheric composition (Seinfeld and Pandis, 2016; Faxon and Allen, 2013). In comparison with hydroxyl (OH) radicals, the

so-called atmospheric detergent, the much faster reaction rates of Cl with volatile organic compounds (VOCs), enhance the
20 peroxy radicals (RO_2) formation and, thereby, the production of ozone (O_3) and secondary organic aerosols (SOA) (Qiu et al.,
2019a; Choi et al., 2020). In addition, Cl radicals can also enhance the oxidation of climate-driving gases (such as methane
and dimethyl sulphide) (Saiz-Lopez and von Glasow, 2012). Cl radicals are produced in the atmosphere through photochem-
istry involving heterogeneous reactions of Cl-containing gases and aerosols (Qiu et al., 2019a; Faxon and Allen, 2013). The
major sources of Cl-containing species are anthropogenic activities in continental regions and sea salt aerosols in marine and
25 coastal environments (von Glasow and Crutzen, 2007; Osthoff et al., 2008; Liao et al., 2014; Liu et al., 2017; Thornton et al.,
2010; Gunthe et al., 2021; Zhang et al., 2022). The photolysis of reactive Cl-containing species, such as chlorine gas (Cl_2),
hypochlorous acid (HOCl), nitryl chloride ($ClNO_2$), and chlorine nitrite (ClONO) and the reaction of hydrochloric acid (HCl)
with OH are known to produce Cl radicals in the lower troposphere (Atkinson et al., 2007; Riedel et al., 2014). With the rise in
anthropogenic activities, emissions of Cl-containing species have increased significantly across the globe (Lobert et al., 1999;
30 Zhang et al., 2022), and hence the importance of Cl in local as well as regional atmospheric chemistry has become prominent.

Despite the aforementioned importance, Cl chemistry and associated mechanism, especially heterogeneous reactions in the
lower troposphere, however, are not yet fully understood, and the effects of Cl on atmospheric composition, air quality and
oxidation capacity remain uncertain. Field measurements have revealed high concentrations of Cl species over inland regions
35 in addition to coastal and polar regions (von Glasow and Crutzen, 2007; Osthoff et al., 2008; Liao et al., 2014; Liu et al.,
2017; Thornton et al., 2010), however, quantitative understanding of continental sources remains poorly understood. This is
due to lack of the relevant heterogeneous and gas-phase chemistry in atmospheric photochemical models despite the range of
chemical mechanisms complexity used in 3-D chemistry transport models (Xue et al., 2015; Pawar et al., 2023; Pozzer et al.,
2022). In addition, the chemistry of Cl compounds has been less studied using the laboratory/chamber experiments. Qiu et al.
40 (2019b) showed that due to inadequate representation of heterogeneous Cl chemistry, the Community Multiscale Air Quality
(CMAQ) model underestimated nitrate concentrations during daytime but overestimated during night-time in Beijing, China.
In addition, the uncertainties associated with emission inventories of Cl species, can lead to inaccurate estimation of air com-
position (Zhang et al., 2022; Sharma et al., 2019). For example, Pawar et al. (2023) noticed that even after the inclusion of HCl
emissions from trash burning the levels of nitrate, sulphate, nitrous acid (HONO) etc., still deviated from the observations in
45 Delhi, India, highlighting the need to include emissions from other sectors, such as industries. Few recent studies assessed the
impacts of the gas phase Cl chemistry by including gas phase $ClNO_2$ reactions, for example, Xue et al. (2015) reported about
25 % enhancement in the daytime oxidation of carbon monoxide and VOCs at a coastal site in East Asia. In the same region,
the model predicted a 5-16 % enhancement in peak ozone with $ClNO_2$ ($\approx$50–200 pmol/mol) at a mountain top in Hong Kong,
China (Wang et al., 2016). The measurements of Cl_2 (up to $\approx$450 pmol/mol) and $ClNO_2$ (up to $\approx$ 3.5 nmol/mol) were reported
50 from a rural site in the North China Plain and Cl chemistry was showed to enhance the formation of peroxy radicals (by 15 %)
and O_3 production rate (by 19 %) (Liu et al., 2017).

Nevertheless, the heterogeneous chemistry of Cl species remains poorly represented in models, and often neglected in large scale numerical simulations. For example, in several models, the heterogeneous uptake of N_2O_5 on aqueous aerosols yielded nitric acid (HNO_3) via reaction HET1:

$$N_2O_5(g) + H_2O(aq) \rightarrow 2\,HNO_3(aq) \qquad\qquad (HET1)$$

 However, N_2O_5 uptake on chloride-containing particles can produce $ClNO_2$ (Behnke et al., 1997; Thornton et al., 2010) especially in urban environments with strong NOx emissions (Osthoff et al., 2008; Young et al., 2012). Incorporating heterogeneous mechanism of $ClNO_2$ into the regional models led to 3–12 % increase in O_3 over Northern China (Sarwar et al., 2014; Zhang et al., 2017; Liu et al., 2017). In addition, heterogeneous reactions of Cl-containing species including particulate chloride (pCl^-), Cl_2, $ClNO_2$, chlorine nitrate ($ClNO_3$), and hypochlorous acid (HOCl) are suggested to result in the formation of Cl radicals as well as in recycling of NOx, and HOx (OH, and HO_2) (Ravishankara, 2009; Qiu et al., 2019a; Hossaini et al., 2016; Faxon and Allen, 2013). Very recent measurements suggest a reduction in $ClNO_2$ formation due to the competition of N_2O_5 uptake among chloride, sulphate and acetate aerosols (Staudt et al., 2019). These heterogeneous reactions can be of paramount significance in the Cl budget, however, to the best of our knowledge, these are not yet considered in model simulations.

The main goal of the present study is to investigate the role of chlorine chemistry in chemically contrasting urban environments. In this regard, we incorporate comprehensive gas-phase and heterogeneous Cl chemistry into a state of the art box model. Section 2 provides a detailed description of the Cl chemistry mechanism with gas-phase and heterogeneous reactions. Section 3 describes the model setup and Section 4 shows the simulation results which include a detailed investigation on (i) the sensitivity of air composition to chlorine chemistry, (ii) the production and loss of Cl and $ClNO_2$, (iii) the role of Cl in the Atmospheric Oxidative Capacity (AOC), and (iv) the sensitivity to $ClNO_2 + Cl^-$ reaction.

2   Mechanism Development

The community box model "Chemistry As A Boxmodel Application/Module Efficiently Calculating the Chemistry of the Atmosphere" (CAABA/MECCA, Sander et al., 2019), has been used in this work. A comprehensive gas- and aqueous-phase mechanism of chlorine chemistry has been added to MECCA, here used within the box model CAABA. The gas-phase and heterogeneous chemistry implemented in MECCA is described in the following subsections and the full mechanism is shown in the supplementary section.

2.1   Gas-phase chlorine chemistry

A total of 36 inorganic, organic and photolysis reactions which are key contributors of Cl radicals were added to the mechanism (Table 1). The mechanism includes the inorganic reactions of Cl with NOx, NO_3 (G1–G4), the reactions of Cl-containing species with OH and NO (G5–G7), and the reactions between Cl-containing species (G8–G9) (Qiu et al., 2019a; Burkholder et al., 2015; Atkinson et al., 2007). ClONO is formed through reaction of Cl with NO_2 (G2), and exists as a metastable

intermediate (Janowski et al., 1977; Niki et al., 1978; Golden, 2007). This intermediate subsequently transforms into $ClNO_2$

85   (G10), with an average conversion time of $\approx$12 h (ranging from 4 to 20 h), and the corresponding rate constant is 2.3 E-5 s^{-1} (Janowski et al., 1977). The Cl-initiated oxidation of organic species i.e. alkanes (C_3H_8, C_4H_{10}), aromatics (benzene (C_6H_6), toluene (C_7H_8) and xylene (C_8H_{10})), alcohols (CH_3OH, C_2H_5OH), ketones (CH_3COCH_3, MEK), isoprene (C_5H_8), and other organic compounds (C_2H_5CHO, $HOCH_2CHO$, BENZAL, GLYOX, MGLYOX) have also been included (G11– G31). The corresponding kinetic data are based on the International Union of Pure and Applied Chemistry and NASA Jet

90   Propulsion Laboratory data evaluations (Atkinson et al., 2006, 2007; Burkholder et al., 2015), and from the literature (Niki et al., 1985, 1987; Green et al., 1990; Shi and Bernhard, 1997; Sokolov et al., 1999; Thiault et al., 2002; Wang et al., 2005; Rickard, 2009; Wennberg et al., 2018). In addition, photolysis reactions (G32–G36) resulting in production of Cl are also added to the module (Atkinson et al., 2007). The abbreviations of species mentioned in Table 1 are kept similar to that in the Master Chemical Mechanism (MCM) nomenclature (Rickard, 2009).

Table 1: Gas-phase chlorine reactions and corresponding rate constants added to MECCA. The rate constants are expressed in units of cm^3 molecule^{-1} s^{-1} unless otherwise specified. Model-simulated maximum noontime J-values for Delhi are provided.

Reaction		Rate constant	Reference
Inorganic reactions			
(G1)	$Cl + NO + M \rightarrow ClNO$	7.6E(-32)*(T/300)$^{-1.8}$	Qiu et al. (2019a)
(G2)	$Cl + NO_2 + M \rightarrow ClONO$	1.6E-11	Burkholder et al. (2015)
(G3)	$Cl + NO_2 + M \rightarrow ClNO_2$	3.6E-12	Burkholder et al. (2015)
(G4)	$Cl + NO_3 \rightarrow ClO + NO_2$	2.40E-11 Qiu et al. (2019a)	
(G5)	$Cl_2 + OH \rightarrow HOCl + Cl$	3.6E-12*exp(-1200/T)	Atkinson et al. (2007)
(G6)	$ClNO_2 + OH \rightarrow HOCl + NO2$	2.4E-12*exp(-1250/T)	Atkinson et al. (2007)
(G7)	$OClO + NO \rightarrow NO_2 + ClO$	1.1E-13*exp(350/T)	Atkinson et al. (2007)
(G8)	$Cl + Cl_2O \rightarrow Cl_2 + ClO$	6.2E-11*exp(130/T)	Atkinson et al. (2007)
(G9)	$ClO + OClO + M \rightarrow Cl_2O_3$	1.2E-12	Atkinson et al. (2007)
(G10)	$ClONO \rightarrow ClNO_2$	2.3E-5 s^{-1}	Janowski et al. (1977)
Organic reactions			
(G11)	$Cl + C_3H_8 \rightarrow iso\text{-}C_3H_7O_2 + HCl$	1.4E-10*0.43*exp(75/T)	Rickard (2009)
(G12)	$Cl + C_3H_8 \rightarrow n\text{-}C_3H_7O_2 + HCl$	1.4E-10*0.59*exp(-90/T)	Rickard (2009)
(G13)	$Cl + iso\text{-}C_4H_{10} \rightarrow iso\text{-}C_4H_9O_2 + HCl$	1.43E-10*0.564	Rickard (2009)
(G14)	$Cl + iso\text{-}C_4H_{10} \rightarrow tert\text{-}C_4H_9O_2 + HCl$	1.43E-10*0.436	Rickard (2009)
(G15)	$Cl + n\text{-}C_4H_{10} \rightarrow LC_4H_9O_2 + HCl$	2.05E-10	Atkinson et al. (2006), Rickard (2009)
(G16)	$Cl + benzene \rightarrow C_6H_5O_2 + HCl$	1.3E-16	Sokolov et al. (1999)

(G17)	Cl + toluene → $C_6H_5CH_2O_2$ + HCl	6.20E-11	Wang et al. (2005)
(G18)	Cl + isoprene → .63 LISOPAB + .30 LISOPCD + .07 LISOPEFO2 + HCl	7.6E-11*exp(500/T)*1.1*exp(-595/T)	Wennberg et al. (2018)
(G19)	Cl + isoprene → .63 LISOPAB + .30 LISOPCD + .07 LISOPEFO2 + LCHLORINE	7.6E-11*exp(500/T)*(1-1.1*exp(-595/T))	Wennberg et al. (2018)
(G20)	Cl + xylene → $C_6H_5CH_2O_2$ + LCARBON + HCl	1.50E-10	Shi and Bernhard (1997)
(G21)	Cl + CH_3OH → $HOCH_2O_2$ + HCl	7.1E-11*0.59*exp(-75/T)	Atkinson et al. (2006)
(G22)	Cl + C_2H_5OH → $HOCH_2CH_2O_2$ + HCl	6.0E-11*exp(155/T)*0.28*exp(-350/T)	Atkinson et al. (2006)
(G23)	Cl + C_2H_5OH → $C_2H_5O_2$ + HCl	6.0E-11*exp(155/T)*(1-0.28*exp(-350/T))	Atkinson et al. (2006)
(G24)	Cl + $HOCH_2CHO$ → HOCHCHO + HCl	8.0E-12/0.9*0.35	Atkinson et al. (2006), Niki et al. (1987)
(G25)	Cl + $HOCH_2CHO$ → $HOCH_2CO$ + HCl	8.0E-12/0.9*(1-0.35)	Atkinson et al. (2006), Niki et al. (1987)
(G26)	Cl + GLYOX → HCOCO + HCl	3.8E-11	Niki et al. (1985)
(G27)	Cl + MGLYOX → CH_3CO + CO + HCl	4.8E-11	Green et al. (1990)
(G28)	Cl + C_2H_5CHO → $C_2H_5CO_3$ + HCl	1.3E-10	Atkinson et al. (2006)
(G29)	Cl + CH_3COCH_3 → $CH_3COCH_2O_2$ + HCl	1.5E-11*exp(-590/T)	Atkinson et al. (2006)
(G30)	Cl + MEK → $LMEKO_2$ + HCl	3.05E-11*exp(80/T)	Atkinson et al. (2006)
(G31)	Cl + BENZAL → $C_6H_5CO_3$ + HCl	1.0E-10	Thiault et al. (2002)
Photolysis reactions		**J-value (s^{-1})**	
(G32)	ClO → Cl + O3P	1.45E-4	Atkinson et al. (2007)
(G33)	Cl_2O → Cl + ClO	9.20E-4	Atkinson et al. (2007)
(G34)	Cl_2O_3 → ClO + ClO_2	5.50E-4	Atkinson et al. (2007)
(G35)	ClNO → Cl + NO	2.89E-3	Atkinson et al. (2007)
(G36)	ClONO → Cl + NO_2	3.81E-3	Atkinson et al. (2007)

2.2 Heterogeneous chemistry

The aqueous-phase and heterogeneous chemistry of Cl compounds added to the MECCA is described in Table 2. In the present study, we assume that N_2O_5 is in equilibrium between the gas- and aqueous-phase (H2) according to Henry's law and the dissociation of $N_2O_5(aq)$ to nitronium ion (NO_2^+) and nitrate (NO_3^-), occurs according to reaction (A1). The rate constant for the recombination reaction of NO_2^+ and NO_3^- is 2.7×10^8 mol^{-1} L s^{-1}, calculated based on Bertram and Thornton (2009);

100 Staudt et al. (2019). The acid dissociation of nitric acid (HNO$_3$) in aqueous phase (A3) also results in formation of NO$_2^+$ (Sapoli et al., 1985).

Table 2: Aqueous-phase and heterogeneous chlorine reactions added to MECCA

Reaction		Rate constant	Reference
Aqueous-phase reactions			
(A1)	N$_2$O$_5$(aq) $\rightarrow$ NO$_2^+$(aq) + NO$_3^-$(aq)	1.5×10^5 s^{-1}	Staudt et al. (2019)
(A2)	NO$_2^+$(aq) + NO$_3^-$(aq) $\rightarrow$ N$_2$O$_5$(aq)	2.7×10^8 mol^{-1} L s^{-1}	Bertram and Thornton (2009); Staudt et al. (2019)
(A3)	HNO$_3$(aq) + H$^+$(aq) $\rightarrow$ NO$_2^+$(aq) + H$_2$O(aq)	1.6×10^9 mol^{-1} L s^{-1}	Sapoli et al. (1985)
(A4)	NO$_2^+$(aq) + Cl$^-$(aq) $\rightarrow$ ClNO$_2$(aq)	7.5×10^9 mol^{-1} L s^{-1}	Staudt et al. (2019)
(A5)	ClNO$_2$(aq) $\rightarrow$ NO$_2^+$(aq) + Cl$^-$(aq)	2.70×10^2 s^{-1}	Behnke et al. (1997)
(A6)	ClNO$_2$(aq) + Cl$^-$(aq) $\rightarrow$ Cl$_2$(aq) + NO$_2^-$(aq)	10^7 mol^{-1} L s^{-1}	Roberts et al. (2008)
(A7)	OH·Cl$^-$(aq) + OH·Cl$^-$(aq) $\rightarrow$ Cl$_2$(aq) + 2 OH$^-$(aq)	1.8×10^9 mol^{-1} L s^{-1}	Knipping et al. (2000)
(A8)	OH·Cl$^-$(aq) + Cl$^-$(aq) $\rightarrow$ Cl$_2^-$(aq) + 2 OH$^-$(aq)	10^4 mol^{-1} L s^{-1}	Grigorev et al. (1987)
(A9)	Cl$_2^-$(aq) + 2 OH$^-$(aq) $\rightarrow$ OH·Cl$^-$(aq) + Cl$^-$(aq)	4.5×10^7 mol^{-1} L s^{-1}	Grigorev et al. (1987)
(A10)	NO$_2^+$(aq) + H$_2$O(aq) $\rightarrow$ HNO$_3$(aq) + H$^+$(aq)	1.6×10^7 mol^{-1} L s^{-1}	Staudt et al. (2019)
(A11)	NO$_2^+$(aq) + SO$_4^{2-}$(aq) $\rightarrow$ SO$_4^{2-}$(aq) + NO$_3^-$(aq) + 2 H$^+$(aq)	7.5×10^9 mol^{-1} L s^{-1}	Staudt et al. (2019)
(A12)	NO$_2^+$(aq) + HCOO$^-$(aq) $\rightarrow$ HCOO$^-$(aq) + NO$_3^-$(aq) + 2 H$^+$(aq)	7.5×10^9 mol^{-1} L s^{-1}	Staudt et al. (2019)
(A13)	NO$_2^+$(aq) + CH$_3$COO$^-$(aq) $\rightarrow$ CH$_3$COO$^-$(aq) + NO$_3^-$(aq) + 2 H$^+$(aq)	7.5×10^9 mol^{-1} L s^{-1}	Staudt et al. (2019)
(A14)	NO$_2^+$(aq) + phenol(aq) $\rightarrow$ HOC$_6$H$_4$NO$_2$(aq) + H$^+$(aq)	7.5×10^9 mol^{-1} L s^{-1}	Ryder et al. (2015); Heal et al. (2007)
(A15)	NO$_2^+$(aq) + CH$_3$OH(aq) $\rightarrow$ CH$_3$NO$_3$(aq) + H$^+$(aq)	4.5×10^8 mol^{-1} L s^{-1}	Iraci et al. (2007)
(A16)	NO$_2^+$(aq) + CRESOL(aq) $\rightarrow$ TOL1OHNO2(aq) + H$^+$(aq)	7.5×10^9 mol^{-1} L s^{-1}	Coombes et al. (1979)
Heterogeneous reactions		**Henry's constant (mol L^{-1} atm^{-1})**	
(H2)	N$_2$O$_5$(g) $\rightleftharpoons$ N$_2$O$_5$(aq)	8.8E-2	Fried et al. (1994)
(H3)	ClNO$_2$(g) $\rightleftharpoons$ ClNO$_2$(aq)	4.5E-2	Frenzel et al. (1998)

(H4)	$HOC_6H_4NO_2(aq) \rightleftharpoons HOC_6H_4NO_2(g)$	8.9E1	Müller and Heal (2001)
(H5)	$CH_3NO_3(aq) \rightleftharpoons CH_3NO_3(g)$	2.0E0	Sander (2015)
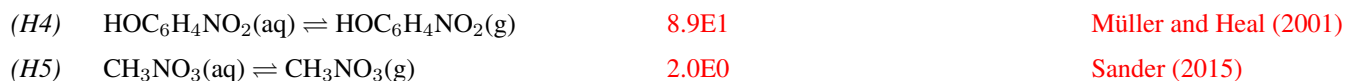
Thus produced nitronium ion (NO_2^+) reacts reversibly with chloride (Cl^-) yielding $ClNO_2$ (A4, A5) (Staudt et al., 2019; Behnke et al., 1997). After outgassing according to Henry's law (H3), $ClNO_2$ is photolyzed in the gas phase, producing Cl and NO_2 (Ghosh et al., 2012; Sander et al., 2014). $ClNO_2$ uptake on chloride containing aerosols results in formation of Cl_2 and nitrite ion (NO_2^-), as shown by the reaction (A6) (Roberts et al., 2008). Chamber experiments suggest the formation of Cl_2 from the self reaction of $OH \cdot Cl^-$ (A7), which gets formed via the reaction of OH with Cl^- (Knipping et al., 2000). Through other channel of reversible reactions (A8, A9), $OH \cdot Cl^-$ reacts with aqueous chloride and produces Cl_2^-, which can yield Cl_2 through subsequent reactions (Grigorev et al., 1987). The NO_2^+ uptake on aqueous chloride to form $ClNO_2$ (A4) is $\approx$500 times faster than NO_2^+ reaction with H_2O (A10) (Staudt et al., 2019). At the same time, experimental studies revealed a strong competition of NO_2^+ to react with Cl^- and with other nucleophiles (e.g. SO_4^{2-}) and aqueous organic compounds e.g. phenol, methanol, cresol (A11–A16) (Staudt et al., 2019; Ryder et al., 2015; Heal et al., 2007; Iraci et al., 2007; Coombes et al., 1979). These reactions could suppress the formation of $ClNO_2$ and also the corresponding rate constants for reactions A11–A14 are similar to the $NO_2^+ + Cl^-$ reaction yielding $ClNO_2$ i.e. 7.5×10^9 mol^{-1} L s^{-1} (Staudt et al., 2019; Ryder et al., 2015; Heal et al., 2007). Methanol reacts with NO_2^+ (A15) and forms aqueous methyl nitrate (CH_3NO_3) (Iraci et al., 2007). Phase exchange for CH_3NO_3 and nitrophenol ($HOC_6H_4NO_2$) is shown by reactions H4 and H5, respectively. Above discussed heterogeneous chemistry implemented in MECCA is summarized in Fig. 1. The rate constant for NO_2^+ reaction with methoxyphenol is about $\approx$10000 times smaller than NO_2^+ + phenol reaction (Kroflič et al., 2015), so it is not considered in this study. In addition, nitration reactions of other alcohols (e.g. catechol and polyphenols) could be potentially important, however due to unavailability of corresponding rate constants, these reactions are not considered in this study, nonetheless future studies calculating the kinetics of these reactions are recommended.
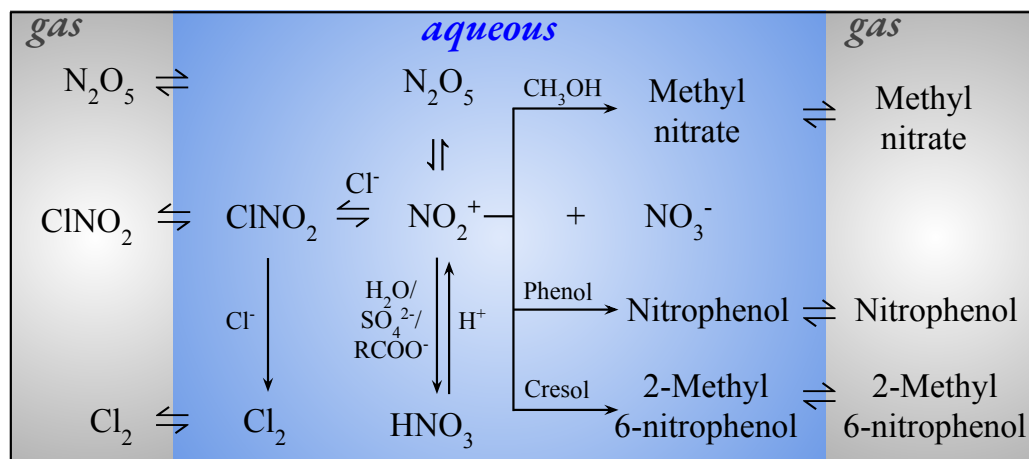
Figure 1. Aqueous-phase and heterogeneous chemistry added to MECCA.

120 In this study, Cl reacts with hydrocarbons and acetone via H-abstraction, and hence does not lead to the formation of any Cl-containing molecules, such as chloroacetone. This means that there are no such reactions in MECCA in which the Cl atom becomes part of the organic molecule. Therefore, for future research, it would be valuable to investigate the chemical kinetics of such reactions kinetics and their importance in the formation of organohalogen compounds.

3 Box model setup

125 The chemistry described in section 2 has been added into community box model CAABA/MECCA v4.4.2 (Sander et al., 2019). A comprehensive gas and aqueous phase tropospheric chemistry involving total 3330 reactions was utilized for the simulations, and the full set of reactions are presented in the electronic supplement. The gas-phase chemistry of organics like terpenes and aromatics is treated by the Mainz Organic Mechanism (MOM) (Taraborrelli et al., 2012; Nölscher et al., 2014; Hens et al., 2014; Taraborrelli et al., 2021). The aqueous-phase chemistry of oxygenated VOCs is treated by the Jülich Atmospheric Mechanism

130 of Organic Chemistry (JAMOC) (Rosanka et al., 2021). The numerical integration of the chemical mechanism is performed by the kinetic preprocessor v2.1 (KPP) (Sandu and Sander, 2006). The photolysis rate constants (*J* values) are calculated by the submodel JVAL, based on the method by Landgraf and Crutzen (1998). The Cl chemistry is expected to be more prominent during winter conditions due to higher concentration of Cl-containing species in the boundary layer (Thornton et al., 2010; Gunthe et al., 2021; Sommariva et al., 2021), and therefore, simulations are performed for the winter season. Hence, the model

135 is set-up for typical winter conditions of two different urban environments: Delhi (28.6° N, 77.2° E), India and Leicester (52.4° N, 01.1° W), United Kingdom. Simulations are performed for a 5-day period (17–21 February 2018) and output of 5th day has been considered for the analysis; by then, radicals had achieved almost a steady state. The typical environmental conditions used in the simulations for Delhi (Tripathi et al., 2022) and Leicester (Sommariva et al., 2021) are summarized in Tab. 3 and Tab. S1.

Table 3. Environmental conditions of Delhi and Leicester in the model simulations.

Parameter	Delhi	Leicester
Latitude	28.58° N	52.38° N
Longitude	77.22° E	01.08° W
Time-zone	GMT+5:30	GMT+0:00
Temperature (K)	292	278.1
Pressure (mbar)	1010	1004
Air number density (molecules cm^{-3})	2.5×10^{19}	2.61×10^{19}
Relative Humidity	67 %	90 %

140 VOC emissions are taken from the CAMS inventory (Sindelarova et al., 2014; Granier et al., 2019) and are adjusted iteratively in magnitude for better agreement with observations. CAMS-GLOB-ANT v5.3 (0.1° × 0.1°) (Granier et al., 2019) provides emissions of anthropogenic VOCs (e.g., benzene, toluene etc.), while emissions of biogenic VOCs (e.g., isoprene) are from CAMS-GLOB-BIO v3.1 (0.25° × 0.25°) (Sindelarova et al., 2014). Emission of HCl and particulate chloride are included from Zhang et al. (2022) and adjusted iteratively towards reported levels of Cl-containing species (Gunthe et al., 2021;

145 Sommariva et al., 2021). The Mainz Organic Mechanism (MOM) dry deposition scenario (Sander et al., 2019) is activated in the model. Ground-based lidar measurements of boundary layer height (BLH) during winter-time, performed as a part of the European Integrated project on Aerosol Cloud Climate and Air Quality Interactions (EUCAARI) project, are utilized for the simulations at Delhi (Nakoudi et al., 2018). The diurnal variation in BLH in Leicester is extracted from the European centre for medium-range weather forecast's (ECMWF) fifth-generation reanalysis dataset ERA5 (Hersbach et al., 2020). Air compo-

150 sition in the model has been initialized based on previous studies (Tab. S1; Zhang et al. (2007); Lanz et al. (2010); Lawler et al. (2011); Sommariva et al. (2018, 2021); Gunthe et al. (2021); Tripathi et al. (2022)). The values of aerosol properties (e.g., radius, liquid water content, and chemical composition) incorporated in the simulations for both Delhi and Leicester as provided in Table. S1. We constrained the model with the parameterized function best representing the observed diurnal variations of NOx (Fig. 2) (Tripathi et al. (2022); Sommariva et al. (2018, 2021), https://uk-air.defra.gov.uk/data/) which helped in better

155 reproducing the diurnal variations of some VOCs (e.g. isoprene) and ozone. Diurnal observations of HONO from Sommariva et al. (2021) are used for Leicester. For Delhi, however, HONO couldn't be constrained due to lack of observations.

4   Results and Discussion

The model captures the patterns in O_3 variability at both locations (Sommariva et al., 2018; Nelson et al., 2021; Chen et al., 2021; Sommariva et al., 2021; Nelson et al., 2023) to an extent, as shown in Fig. 2. O_3 is underestimated after ≈16:00 h LT

160 in Leicester mainly due to titration by high NO and lack of adequate dynamics/transport of O_3 in the model. Entrainment seems to improve O_3 after mid-night, towards the observed values (Fig. 2i). Simulated isoprene is in agreement with diurnal observations in Delhi (Tripathi et al., 2022) and in accordance with observed mean level in Leicester (Sommariva et al., 2021). The nitrate radical (NO_3), which is a nighttime oxidant, is formed through reaction between NO_2 and O_3 (G37). NO_3 can react with NO_2 forming N_2O_5, which can again produce NO_3 and NO_2 through thermal dissociation (G38).

165 $$NO_2 + O_3 \longrightarrow NO_3 + O_2 \tag{G37}$$

$$NO_3 + NO_2 + M \rightleftharpoons N_2O_5 + M \tag{G38}$$

As seen in Fig. 2e, NO_3 remains negligible during the night-time (≈18:00–07:30 h LT) in Delhi due to unavailability of O_3 under high-NO conditions (up to 200 nmol/mol). Interestingly, despite its very short lifetime (≈5 s), about ≈0.1 pmol/mol of NO_3 sustains during daytime. This is primarily due to prevailing levels of NO_2 (≈30 nmol/mol) and O_3 (≈40 nmol/mol).

170 Such unusual daytime enhanced NO_3 have been reported in recent studies, for example, 5-31 pmol/mol of NO_3 in Texas, USA
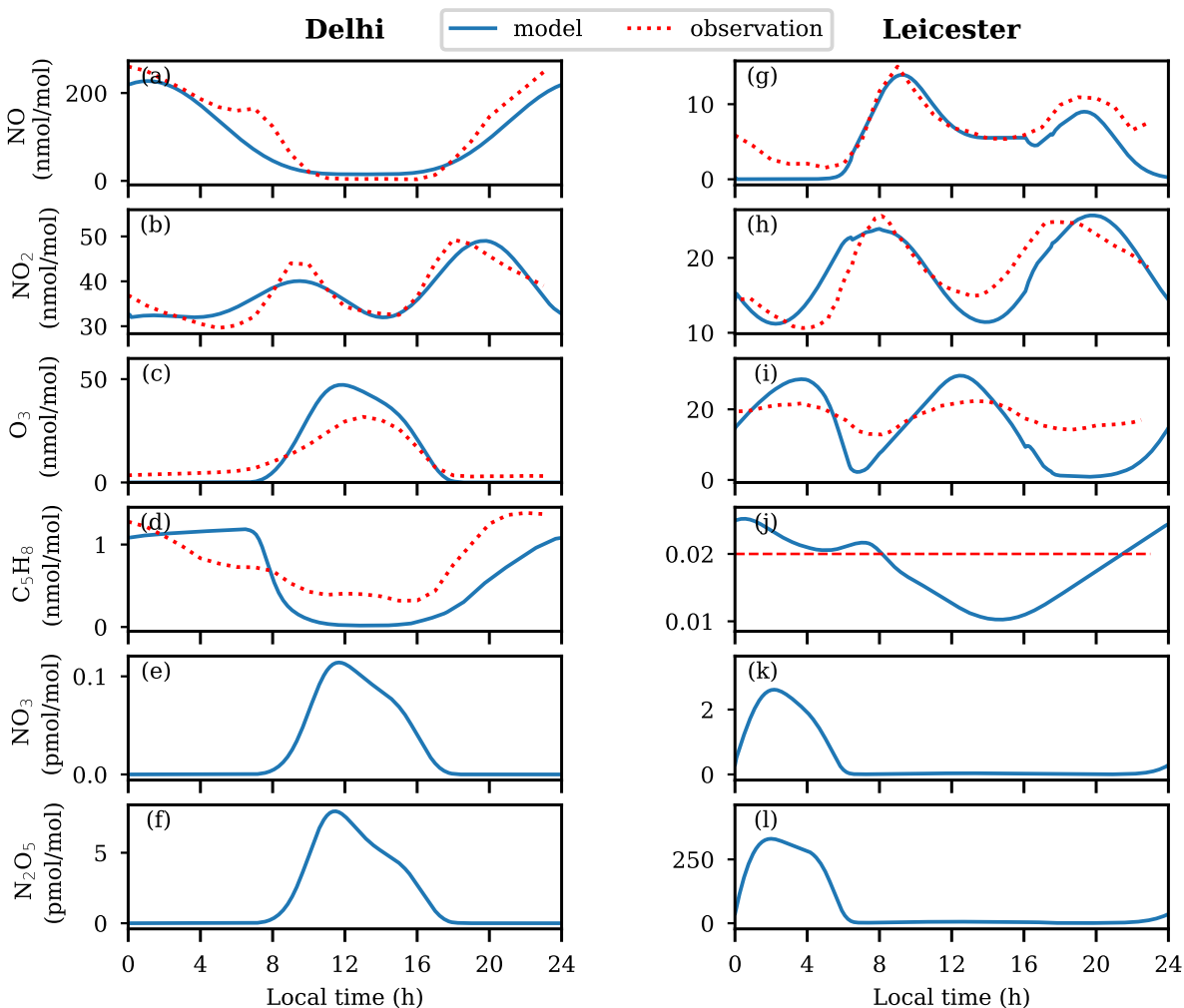
Figure 2. Diurnal variations of $NO, NO_2, O_3, C_5H_8, NO_3$, and N_2O_5 mixing ratios in Delhi (left) and Leicester (right). The unusal and negligible nighttime NO_3 in Delhi is attributed to the nearly non-existent O_3, due to titration by higher concentrations of NO. This leads to the negligible nighttime N_2O_5 in this region. Although mixing ratios of NO_3 and N_2O_5 peak during the daytime, their levels remain quite low. Mean value of observed C_5H_8 in Leicester is shown by red colored long dashed line.

(Geyer et al., 2003). Aircraft measurements during the New England Air Quality Study showed ≈0.5 pmol/mol of NO_3 within boundary layer (≤1 km) during noon time (Brown et al., 2005). The calculated NO_3 levels using steady state approximation showed 0.01-0.06 pmol/mol of NO_3 for the 1997-2012 period at urban sites in the UK (Marylebone Road London, London Eltham, and Harwell) (Khan et al., 2015a). Horowitz et al. (2007) suggested that NO_3 in tenths of pmol/mol during daytime over the eastern United States results in formation of ≈50 % isoprene nitrates through oxidation of isoprene, which could further affect the formation of O_3 and SOA significantly (Horowitz et al., 2007). Following to higher NO_3, up to 8 pmol/mol

of N_2O_5 is simulated during daytime in Delhi (Fig. 2f). Similar unusual daytime high levels of N_2O_5 ($\approx21.9\pm29.3$ pptv) during wintertime were recently measured at Delhi using a high-resolution iodide adduct chemical ionization mass spectrometer (Haslett et al., 2023).

180

Enhanced $NO_3 \approx 2.6$ pmol/mol and $N_2O_5 \approx 330$ pmol/mol are simulated after mid-night in Leicester (Fig. 2k, 2l). In contrast to Delhi, the daytime simulated levels of NO_3 are negligible as it gets removed fast during the daytime by photolysis and through its reactions with NO, HO_2, RO_2, and VOCs (Khan et al., 2015b). In conjunction with high NO from $\approx16:00$ h LT to near midnight that titrates O_3, the corresponding NO_3 and N_2O_5 is negligible (following reactions G37 and G38). Night-time

185 high and negligible day-time levels of NO_3 and N_2O_5 are their typical features which are generally reported in the literature (Brown et al., 2001; Seinfeld and Pandis, 2016).

4.1 Sensitivity of air composition to chlorine chemistry

To investigate the effects of Cl chemistry on air composition, other than comprehensive chemistry simulation discussed in
190 previous section (simulation: NEW i.e. chemistry already present in the model + newly added gas and aqueous phase chlorine chemistry), two additional simulations have been performed, which are: (1) OLD – this includes default chemistry already present in the model, and (2) NOCL – OLD minus chlorine chemistry (i.e. without Cl chemistry). OLD simulation also encompassed some basic chlorine chemistry that was part of the model prior to its update (full mechanism is also shown in supplement). Figure 3 shows the comparison of Cl, $ClNO_2$, ClONO, OH, HO_2, and RO_2 variations among the three simu-
195 lations in Delhi and Leicester. Figure S5 shows the differences in diurnal variations of Cl, $ClONO + ClNO_2$, OH, HO_2, and RO_2 in NEW simulation with: NOCL and OLD simulations.

The Delhi environment is mainly characterized by two peaks in Cl, a predominant sharp peak just after the sunrise followed by a broad shallow peak during noontime, corresponding to different mechanisms as discussed in the next section. With newly
200 added chemistry (NEW simulation), a sharp peak in Cl is seen near the sunrise, with the maximum values attained is ≈3.5 fmol/mol (8.75×10^4 molec cm^{-3}) in Delhi (Fig. 3a). A broad smaller peak with magnitude of ≈0.8 fmol/mol maximizing around noontime is seen, which is ≈4 times smaller than the first morning peak. OLD simulation also show a sharp peak in Cl near sunrise in Delhi, with a maximum of ≈11 fmol/mol (2.75×10^5 molec cm^{-3}). Cl get suppressed by up to ≈ 0.01 pmol/mol of maximum value in the OLD simulation, in the presence of added chlorine chemistry (NEW) as shown in Fig. S5.
205 Similar to Cl, a peak is seen in $ClONO + ClNO_2$ of ≈100 pmol/mol with sunrise, which gradually decreases and attain ≈7 pmol/mol from nearly 11:00–16:00 h LT. Afterwards it increases to ≈20 pmol/mol from late evening as shown by Fig. 3b,c. The pathways for the formation of $ClNO_2$ and ClONO were absent in earlier version of the model (OLD). Simulated OH, HO_2, and RO_2 show a prominent peak just after sunrise in the presence of Cl chemistry for both the OLD and NEW simulations (Fig. 3d,e,f). As a consequence of greater oxidation of VOCs by Cl, enhanced levels of OH by 0.05 pmol/mol (up to
210 a factor of ≈1.8), HO_2 by 0.21 pmol/mol and RO_2 by 0.1 pmol/mol are noted with added Cl chemistry compared to NOCL
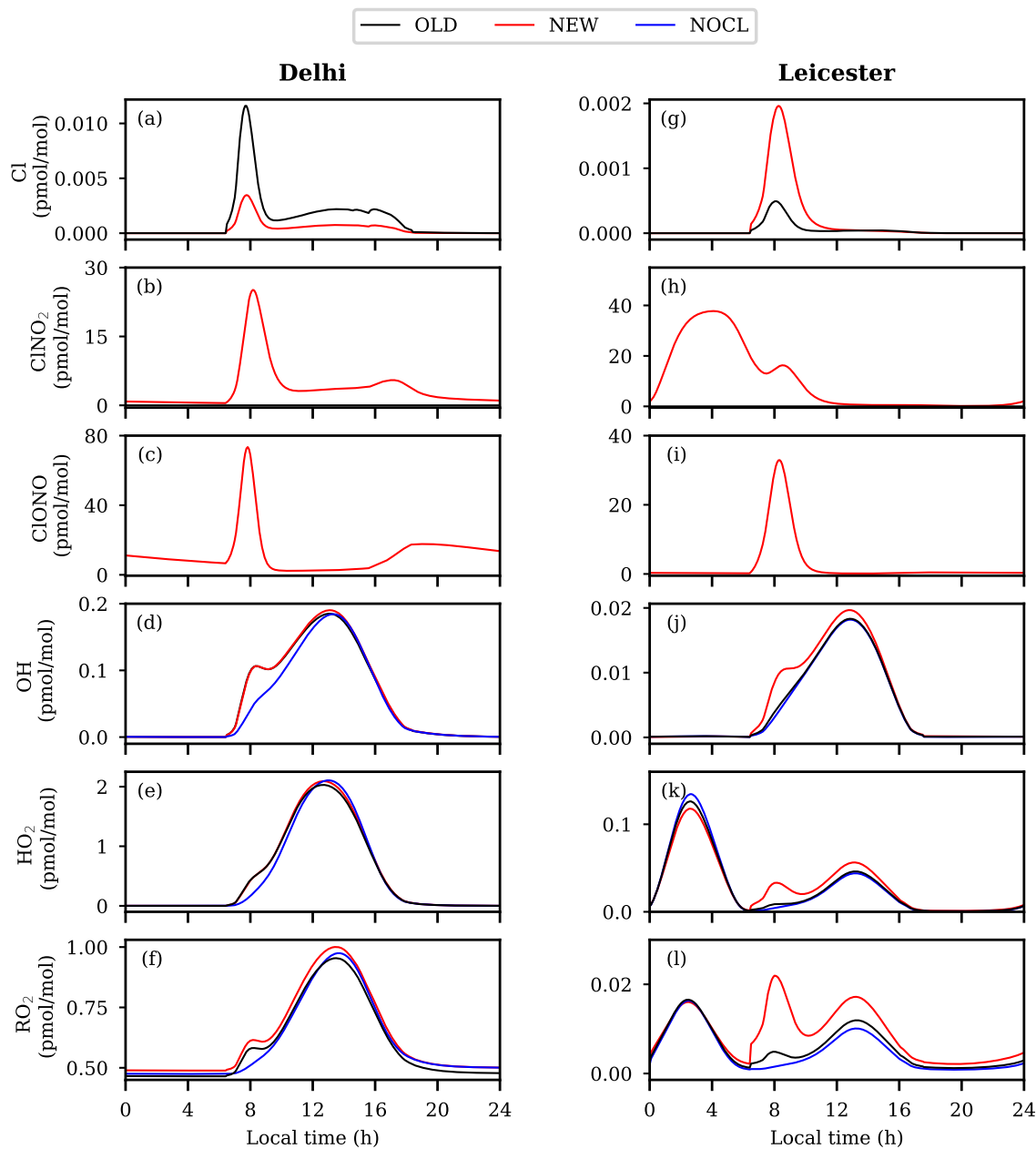
Figure 3. Model simulated diurnal variations of Cl, $ClNO_2$, ClONO, OH, HO_2, and RO_2 at Delhi (left panel) and Leicester (right panel).

case (see Fig. S5). No significant changes are seen in noon-time levels of OH and HO_2, whereas ≈ 1.1 times more RO_2 is produced with added Cl chemistry (NEW) compared to the OLD simulation.

The model-predicted Cl peaks at ≈ 2 fmol/mol (5.2×10^4 molec cm^{-3}) during sunrise in Leicester (Fig. 3g). In contrast to Delhi, suppressed Cl (up to ≈ 3.2 times) with a narrow peak is simulated by OLD simulation in comparison with NEW simulation containing newly added Cl chemistry, at Leicester. In contrast to negligible night-time $ClONO + ClNO_2$ in Delhi, it shows a strong build-up over Leicester during 0-4 hours with a maximum of ≈ 40 pmol/mol, with higher levels (up to 50 pmol/mol) prevailing until about sunrise. $ClONO + ClNO_2$ is negligible during mid-day until mid-night, in accordance with N_2O_5 in Leicester as shown in Fig. 2l. Previous studies have demonstrated that the formation of $ClNO_2$ occurs within the nocturnal residual layer, which contains lower levels of NO compared to the surface layer. Subsequently, $ClNO_2$ mixes downward during the morning when the convective mixed layer develops (Bannan et al., 2015; Tham et al., 2016). However, the present study does not account the the effect of transport processes due to the limitations of the box model. The effects of added Cl chemistry on OH, HO_2, and RO_2 are more prominent in Leicester compared to Delhi. NEW simulation show strong enhancements in OH (up to ≈ 2 times), HO_2 (up to ≈ 5 times), and RO_2 (up to ≈ 8 times) after sunrise which is gradually progressive, resulting in higher levels during noon-time as well (Fig. 3, Fig. S5). Remarkably elevated levels of RO_2 (by a factor of ≈ 2) are prominent during the noon hours. Such elevated levels of RO_2 could favour enhanced levels of secondary organic aerosols in Leicester. The impact of Cl chemistry on aerosols (NO_2^+, NO_3^-, and oxalic acid) is discussed in Supplementary section 2.2 (Fig. S6). Though significant differences in NO_2^+, NO_3^-, and oxalic acid are seen due to Cl chemistry but further measurements are required for validation. In the next sections, we have analysed the observed behaviour of Cl and $ClNO_2$ in the NEW simulation over both the locations in more detail.

4.2 Production and loss of Cl and $ClNO_2$

The sources and sinks of Cl in Leicester and Delhi are presented in Fig. 4. The left-upper panels (a) delineates the sources and sinks of Cl radical on diurnal scale in Delhi. The morning sharp peak in Cl radical is caused mainly by the photolysis of Cl_2 with a maximum rate of 1.2×10^7 molec cm^{-3} s^{-1}. The shallow secondary peak is due to the reaction $HCl + OH$ with a noon time rate of $\approx 0.4 \times 10^7$ molec cm^{-3} s^{-1}. However, there is a smaller contribution from other reactions (photolysis of $ClNO_2$, ClONO and reaction of ClO with NO) to the morning peak, while have negligible contributions during the daytime. Interestingly, there is a strong consumption of Cl to oxidize VOCs (peak rate $\approx 2.4 \times 10^7$ molec cm^{-3} s^{-1}) during sunrise, and a lesser consumption during the rest of the day. $Cl + NO_2$ is also a Cl sink during the morning time in Delhi. The Cl-initiated oxidation of VOCs in the morning hours in Delhi may lead to formation of secondary organic aerosols and new particle formation, which opens up pathways of future research in this direction. In addition to Cl_2 photolysis ($\approx 1.0 \times 10^6$ molec cm^{-3} s^{-1}), photolysis of $ClNO_2$ and ClONO, and $ClO + NO$ reaction (total rate $\approx 0.8 \times 10^6$ molec cm^{-3} s^{-1}) are other prominent sources of Cl in Leicester. VOCs are the major sink for Cl (rate $\approx 1.3 \times 10^6$ molec cm^{-3} s^{-1}), followed by NO_2 (rate $\approx 0.6 \times 10^6$ molec cm^{-3} s^{-1}).

We further analyzed the production and loss pathways of $ClNO_2$, as shown in Fig. 4c,d. While the major source of $ClNO_2$ is through the $Cl + NO_2$ reaction with a reaction rate $\approx 3 \times 10^5$ molec cm^{-3} s^{-1} in Delhi, the aqueous phase reaction $Cl^- + NO_2^+$ ($\approx 3.4 \times 10^5$ molec cm^{-3} s^{-1}) is the prominent source in Leicester corresponding to the peak $ClNO_2$ (Fig. 2h,p). Though gas-
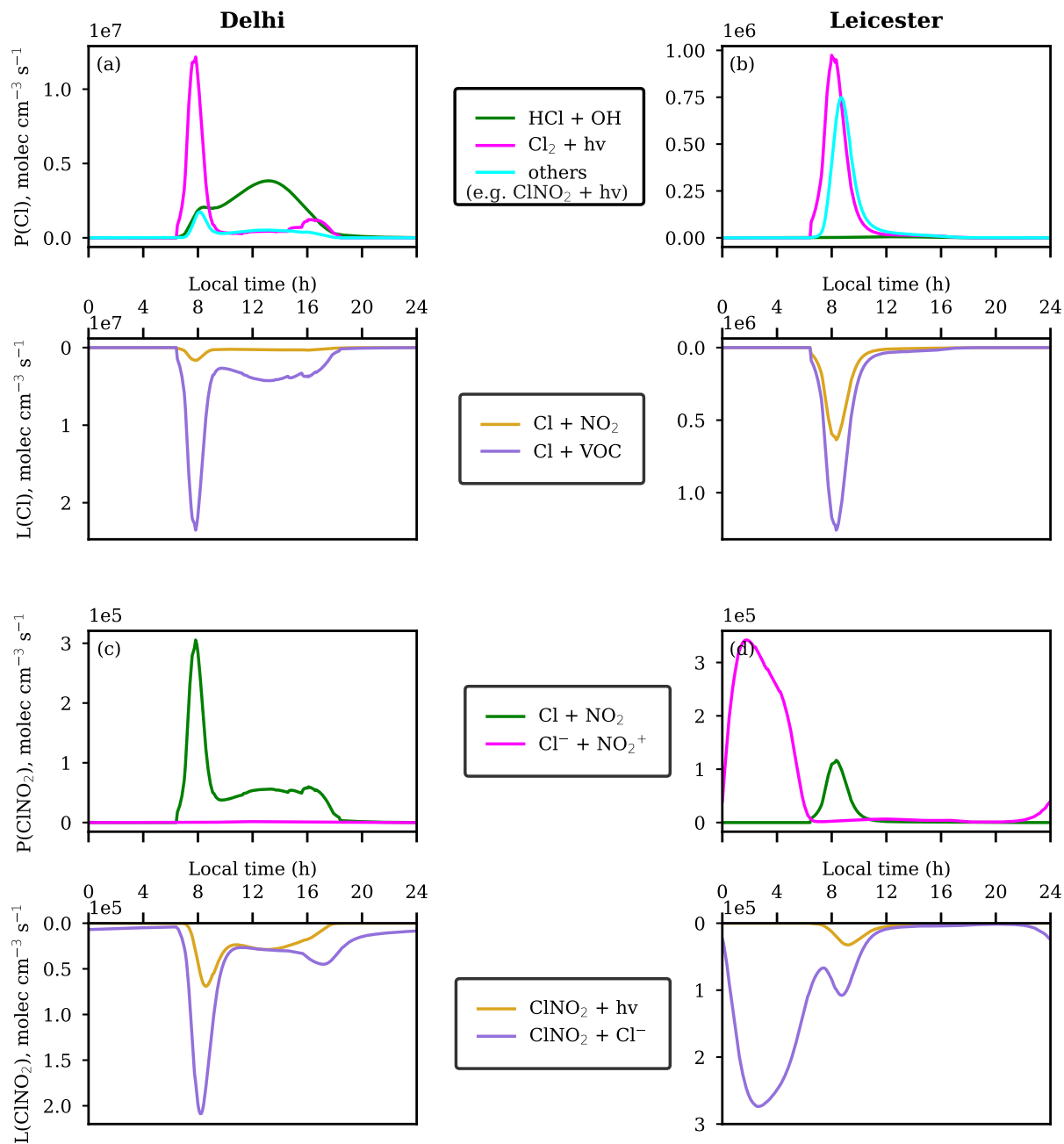
Figure 4. Production and loss rates of (a, b) Cl and (c, d) $ClNO_2$ in Delhi (left panel) and Leicester (right panel).

phase reaction $Cl + NO_2$ is discussed in the literature (Burkholder et al., 2015; Qiu et al., 2019a), however, to the best of our knowledge, such an unusually higher contribution of this reaction (seen in Delhi) as compared to the aqueous-phase reaction

250 of $Cl^- + NO_2^+$ has not been reported in any study. The reaction of Cl with NO_2 ($\approx 1.1 \times 10^5$ molec cm^{-3} s^{-1}) is the major $ClNO_2$ source during the sunrise in Leicester. In contrast, there is lesser contribution of $Cl^- + NO_2^+$ reaction (rate $\approx 1 \times 10^3$ molec cm^{-3} s^{-1}) in $ClNO_2$ production in Delhi. The prominent sink for $ClNO_2$ is through it's heterogeneous reaction with Cl^- ($\approx 1.8 \times 10^5$ molec cm^{-3} s^{-1} or 7.2×10^{-15} mol mol^{-1} s^{-1}) in Delhi almost throughout the day, while it's loss through the photolysis ($\approx 0.5 \times 10^5$ molec cm^{-3} s^{-1} or 2×10^{-15} mol mol^{-1} s^{-1}) is also an important sink during the daytime.

255 $ClNO_2$ loss through the reaction $ClNO_2 + Cl^-$ ($\approx 2.7 \times 10^5$ molec cm^{-3} s^{-1} or 1.0×10^{-14} mol mol^{-1} s^{-1}) is its major sink in Leicester from mid-night to mid-day, while photolysis ($\approx 0.3 \times 10^5$ molec cm^{-3} s^{-1} or 1.1×10^{-15} mol mol^{-1} s^{-1}) is smaller sink from sunrise to mid-day here. The diurnal variation in Cl_2, and its production and loss mechanisms over Delhi and Leicester are shown by Fig. S1 and Fig. S2. In conjunction with major loss of $ClNO_2$, $ClNO_2 + Cl^-$ reaction is the major contributor to Cl_2 formation over Delhi and Leicester.

260

We also calculated $ClNO_2$ yield from NO_2^+ (Fig. S3), which is the ratio of P_{ClNO_2}/L_{total}, where P_{ClNO_2} is the rate of $ClNO_2$ production through $Cl^- + NO_2^+$ reaction and L_{total} denotes the loss rate of NO_2^+ through it's reactions with Cl^-, H_2O, SO_4^{2-}, $HCOO^-$, CH_3COO^-, phenol, CH_3OH, and cresol (A4, A10–A16). $ClNO_2$ yield is ≈ 0.9 over Delhi, indicating the strongest loss of NO_2^+ is through it's reaction with Cl^-, which is also mimicked in Fig. S4a showing the same concentrations of $ClNO_2$

265 as in NEW simulation and when other NO_2^+ reactions (A10–A16) are turned off (simulation: without other NO_2^+ reactions). $ClNO_2$ yield over Leicester is between ≈ 0.40-0.55, which is about half the yield in Delhi. Stronger $ClNO_2$ yield in Delhi could be attributed to ≈ 2 times higher Cl^- than Leicester. Lesser $ClNO_2$ yield in Leicester portrays the importance of NO_2^+ loss reactions (A10–A15) other than with Cl^-, which could be seen through Fig. S4b where $ClNO_2$ is increased by more than twice during early morning hours when A10–A15 reactions are kept inactive in the model. The determination of $ClNO_2$ yield

270 using cavity ring-down spectroscopy and chemical ionization mass spectrometry, shows yield ranging between 0.2 to 0.8 for Cl^- concentrations of 0.02 to 0.5 mol/L (Roberts et al., 2009). The measurements of $ClNO_2$ yield for coastal and open ocean waters were found to be between 0.16-0.30 which is suppressed by up to 5 times than equivalent salt containing solutions, due to the addition of aromatic organic compounds (e.g., phenol and humic acid) to synthetic seawater matrices (Ryder et al., 2015).

275 ## 4.3   Role of Cl in Atmospheric Oxidative Capacity (AOC)

In order to understand the role of Cl as oxidising agent with respect to the OH radical, we calculated the reactivity of Cl and OH as $\Sigma_{X_i} (k_{radical+X_i} \times [X_i])$, where radical is Cl or OH, and $[X_i]$ is the concentration of specie X_i (here X_i includes CO, CH_4, primary VOCs and NMHCs which are initialized in the model) (Fig. 5). The corresponding rate constants for $Cl + X$ and $OH + X$ reactions are taken from the MECCA. The reactivity of both Cl and OH decreases rapidly nearly from sunrise

280 to noon time and afterwards increases gradually at both locations. In comparison to Leicester, the magnitudes of Cl and OH reactivity in Delhi are higher by up to ≈ 1.4 and ≈ 12 times, respectively. However, the Cl/OH reactivity ratio in Leicester is up to ≈ 9 times higher than that in Delhi. Cl reactivity is lower (Delhi: ≈ 685 s^{-1}, Leicester: ≈ 553 s^{-1}) during noontime and higher (Delhi: ≈ 750 s^{-1}, Leicester: ≈ 554 s^{-1}) during nighttime and early morning hours at both locations. The OH reactivity

follows a similar pattern as that of Cl in Delhi and Leicester. The ratio of Cl to OH reactivity starts increasing after sunrise, reaching a maximum value of ≈ 42 at nearly 16:00 h LT and then decreases further in Delhi. As mentioned above, Cl/OH reactivity ratio in Leicester shows a double peak pattern, with one peak (≈ 270) during early morning $\approx 04:00$ h LT and other peak (≈ 276) at about 16:00 h LT.
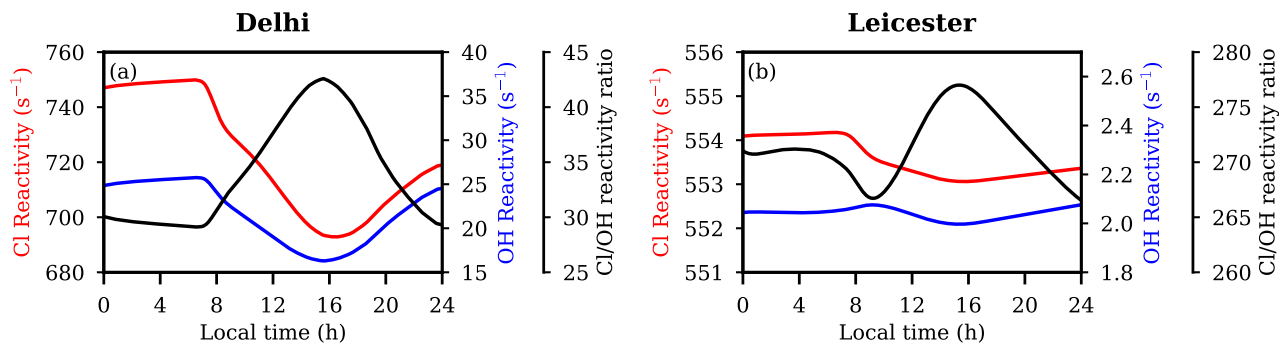
Figure 5. Reactivity of Cl and OH with CO, CH_4, and VOCs, and Cl/OH reactivity ratio during the simulation period in (a) Delhi and (b) Leicester.

We quantified the relative contribution of Cl in atmospheric oxidative capacity (AOC) using the model. AOC represents the sum of oxidation rates of specie X_i by oxidants Y (OH, Cl, and other radicals: NO_3 and O_3) (Elshorbany et al., 2009):

$$AOC = \sum k_{X_i} [X_i][Y] \tag{1}$$

where, k_{X_i} is the corresponding rate constant for X_i + Y reaction. Figure 6 shows the contribution of individual oxidants in AOC at both locations. Besides OH, Cl is the second most important oxidant in Delhi, with a significant contribution of 23.4 % during morning (averaged over 07:00-09:00 h LT), and 8.2 % throughout the day (06:00-16:00 h LT). In Leicester, Cl is the highest contributor (74.0 %) towards AOC during morning. In fact, with 34.1 % contribution, Cl is major oxidant after OH, during the daytime. The higher contribution of Cl in AOC is further substantiated by the ratio of Cl reactivity to OH reactivity (Fig. 5b). This ratio indicates that Cl reactivity exceeds OH reactivity by a significant margin, ranging from 265 to 276 times greater throughout the day in Leicester. Such a substantial contribution of Cl in AOC leads to enhancements of RO_2 as seen in Fig. 3(f,l). Especially, a prominent peak in RO_2 during early morning (07:00-09:00 h LT) is imparted to strong participation of Cl in atmospheric oxidation during this time. Notably strongest contribution of Cl in AOC during early morning in Leicester, strengthens RO_2 peak by up to a factor of 8 (Fig. 3l). The role of Cl is predominant in Leicester as well as in Delhi during early morning, compared to a polluted environment of Hong Kong, China where Cl contribution was estimated to be 21.5 % (Xue et al., 2015). NO_3 and O_3 were found to play a relatively minor role in AOC at both urban environments.
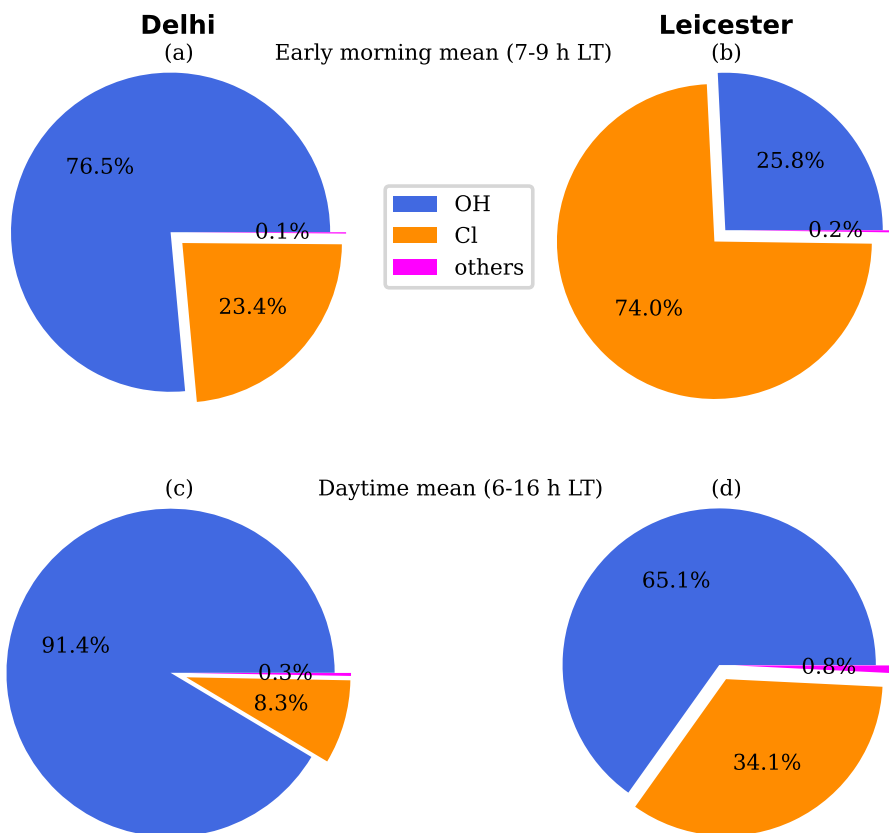
Figure 6. Atmospheric oxidative capacity (AOC) of radicals during (a, b) early morning mean (7-9 h LT) and (c, d) daytime mean (6-16 h LT) in Delhi (left panel) and Leicester (right panel).

4.4 Sensitivity to $ClNO_2$ + Cl^- reaction

In a study conducted by Haskins et al. (2019), using the reacto-diffusive length-scale framework, it was demonstrated that field and laboratory observations could be reconciled by considering an aqueous-phase reaction rate constant for the $ClNO_2$ + Cl^- reaction on the order of $\approx 10^4$ s^{-1}. This reaction rate constant is considerably lower (by $\approx$179 times) than reported in Roberts et al. (2008). In this context, sensitivity simulation (NEWrate) is performed using a reaction rate coefficient of 5.6×10^4 mol^{-1} L s^{-1} (Haskins et al., 2019) for the $ClNO_2$ + Cl^- reaction, for both Delhi and Leicester. As depicted in Figure S7a, the concentration of Cl remains nearly the same in the NEWrate simulation compared to the NEW simulation over Delhi. However, there are significant changes in the concentration of $ClNO_2$, as shown in Fig. S7b. The simulated $ClNO_2$ exhibits a broader peak and is approximately 30 pmol/mol higher near sunrise in the NEWrate simulation when compared to the NEW simulation. During the nighttime, approximately 20 pmol/mol of $ClNO_2$ is simulated in the NEWrate simulation, whereas it is negligible in the NEW simulation (see Fig. 3b). Since the Cl concentration is almost similar in both the NEW and NEWrate

simulations, the differences in the simulated concentrations of OH, HO_2, and RO_2 remain consistent between the NEWrate or NEW simulations and the OLD and NOCL simulations (refer to Fig. S7d, e, f, and Fig. 3d, e, f). The production and loss mechanisms of Cl are similar in both the NEW and NEWrate simulations (see Fig. S8a and Fig. 4a). The contributions from $ClNO_2$ formation reactions are also similar. However, in contrast to the NEW simulation, the loss of $ClNO_2$ through photolysis becomes dominant and is $\approx$6 times greater than its loss through $ClNO_2 + Cl^-$ reaction, in NEWrate simulation. The contribution of radicals to AOC is also similar between the NEW and NEWrate simulation, as depicted in Fig. 6a,c and Fig. S9a,c respectively, over Delhi.

In contrast to Delhi, significant differences are seen in atmospheric composition in Leicester when the rate coefficient of the $ClNO_2 + Cl^-$ reaction is altered (as shown in Fig. S7). The peak concentration of Cl becomes $\approx$0.6 fmol/mol during the morning hours of NEWrate simulation (Fig. S7g), which is about 4 times lower than the concentration of Cl in NEW simulation (Fig. 3g). However, due to slower rate of $ClNO_2$ consumption with Cl^-, the simulated $ClNO_2$ using the NEWrate is significantly enhanced (by $\approx$ 5 times) compared to NEW simulation, reaching a maximum of about 210 pmol/mol around sunrise (see Fig. S7h). Due to lower Cl concentrations, the levels of ClONO also decrease by 3.5 times in NEWrate simulation (as shown in Fig. S7i) compared to NEW simulation (Fig. 3i). The dominant peak seen at sunrise in the NEW simulation for OH, HO_2, and RO_2 is significantly reduced with the lower rate of the $ClNO_2 + Cl^-$ reaction, as illustrated in Fig S7j,k,l. Significant changes in the production and loss mechanisms of Cl and $ClNO_2$ are seen in Leicester when the reaction rate of A6 is changed, as shown in Fig. S8 and Fig. 4b. For example, in the NEWrate simulation, other reactions, including the photolysis of $ClNO_2$ and ClONO, and ClO + NO reaction, become prominent sources of Cl (with a rate of approximately 6.0 x 10^5 molec cm^{-3} s^{-1}), whereas in the NEW simulation, the major source for Cl is photolysis of Cl_2. The primary source for $ClNO_2$ production remains the $Cl^- + NO_2^+$ reaction in both the NEW and NEWrate simulations. However, in the NEWrate simulation, $ClNO_2$ loss from photolysis becomes the major sink, whereas in the NEW simulation, loss from the $ClNO_2 + Cl^-$ reaction is prominent. In addition, remarkable changes in AOC are seen between the NEWrate (Fig. S9b, d) and the NEW simulation (Fig. 6b,d). In the NEWrate simulation, even though Cl remains the major oxidant its contribution is notably reduced from 74% (in NEW simulation) to 58.1% during the early morning hours.

5   Summary and Conclusions

Extended gas- and aqueous-phase chemistry of chlorine compounds has been added to the MECCA mechanism. It consists of 36 gas-phase reactions (inorganic, organic, and photolysis reactions). A total of 24 aqueous-phase and heterogeneous reactions have been added, containing detailed chemistry of N_2O_5 uptake on aerosols to yield $ClNO_2$ and various other competing reactions. The updated model is applied to two different urban environments: Delhi (India) and Leicester (United Kingdom) during winter time. The major conclusions are:

1. The model predicts up to 0.1 pmol/mol of NO_3 and up to 8 pmol/mol of N_2O_5 during daytime in Delhi. However, night-time production of NO_3 and N_2O_5 is seen to be negligible primarily due of the unavailability of O_3. In contrast

to Delhi, NO_3 and N_2O_5 after mid-night in Leicester is ≈ 2.6 pmol/mol and ≈ 330 pmol/mol, respectively. N_2O_5 uptake on aerosols yields $ClNO_2$, which produces Cl via photolysis.

2. A sharp build-up of Cl with sunrise is mainly through Cl_2 photolysis in Delhi. Besides Cl_2, photolysis of $ClNO_2$ and $ClONO$ and the reaction of ClO with NO are prominent Cl sources in Leicester. VOCs are the main sink for Cl at both locations, whereas NO_2 is also an important sink for Cl in Leicester. The latter results in the formation of $ClNO_2$ with a major contribution in Delhi, while $Cl^- + NO_2^+$ is a stronger source in Leicester. Photolysis is the major sink for $ClNO_2$ in Delhi, however, its uptake on chloride aerosols is a prominent sink in Leicester.

3. The magnitude of Cl (≈ 750 s^{-1}) and OH (≈ 25 s^{-1}) reactivities are significantly greater in Delhi, particularly during the morning hours, when compared to Leicester. However, pronounced ratio (≈ 270) of Cl to OH reactivity in Leicester shows a much higher oxidation potential of Cl compared to OH.

4. Sensitivity simulations reveal substantial post-sunrise enhancements of in OH, HO_2, and RO_2 radicals, with a prominent secondary peak due to Cl chemistry. Up to 8 times higher RO_2 is simulated in Leicester primarily because of leading role of Cl in AOC potential.

It is important to note that box models, despite their general limitation of neglecting transport phenomena and assuming species to be well mixed, do include highly detailed chemical mechanisms. Furthermore, because the model is initialized with measurements of chemical species at both locations and the modeled levels align with observed data, significant discrepancies in model estimates would be unexpected. Future studies focussing on modeling vertical gradients, in particular for radical reservoir species such as HONO, and $ClNO_2$ (Young et al., 2012) are recommended.

This study highlights the vital role of Cl chemistry in governing the oxidation capacity of the atmosphere and air quality, and therefore it is important to account for it in detailed photochemical as well as in 3-D chemical transport models. This will lead to better quantify the importance of radicals in atmospheric oxidation and hence, the formation of ozone as well as secondary aerosols, over regional to global scale. Future studies focusing on secondary aerosol formation and new particle formation from heterogeneous reactions are needed to deepen the understanding of transformation of trace gases to aerosols.

Code and data availability. CAABA/MECCA is a community box model published under the GNU General Public Licence, available from the Gitlab repository (https://gitlab.com/RolfSander/caaba-mecca). The version of CAABA/MECCA updated in this study is currently available in the 'delhi' branch of the repository. The new chlorine mechanism will be included in the next release of CAABA/MECCA. All the model outputs associated with this study are archived at zenodo (https://zenodo.org/record/8332131; Soni et al. (2023)).

Author contributions. M. Soni, R. Sander, and D. Taraborrelli designed the study with inputs from S. S. Gunthe, P. Liu, and N. Ojha. M. Soni, R. Sander, and D. Taraborrelli developed and analyzed the chemical mechanism and M. Soni performed the simulations. A. Pozzer,

R. Sander, L. K. Sahu, D. Taraborrelli, I. A. Girach, and N. Ojha helped M. Soni in the analyses and interpretations of the results. A. Patel assisted M. Soni in compiling literature and some input dataset. M. Soni wrote the manuscript and all the co-authors contributed to the review
380 and editing.

Competing interests. The authors declare no conflicts of interest.

Acknowledgements. The authors gratefully acknowledge the use of CAMS inventory for VOCs emissions data available from ECCAD (https://eccad3.sedoo.fr/catalogue). We thank ECMWF for the ERA5 dataset. We acknowledge UK AIR Air Information Resource for the chemical species data through https://uk-air.defra.gov.uk/data/. Authors thank J. M. Roberts (NOAA Chemical Sciences Laboratory, USA),
385 Tao Wang (The Hong Kong Polytechnic University, Hong Kong), Men Xia (University of Helsinki, Finland), and Renuka Soni for valuable inputs on kinetics. M. Soni, N. Ojha, and L. K. Sahu acknowledge support from the Physical Research Laboratory, Ahmedabad, funded by the Department of Space, Government of India.

References

Atkinson, R., Baulch, D. L., Cox, R. A., Crowley, J. N., Hampson, R. F., Hynes, R. G., Jenkin, M. E., Rossi, M. J., Troe, J., and IUPAC Subcommittee: Evaluated kinetic and photochemical data for atmospheric chemistry: Volume II – gas phase reactions of organic species, Atmos. Chem. Phys., 6, 3625–4055, https://doi.org/10.5194/ACP-6-3625-2006, 2006.

Atkinson, R., Baulch, D. L., Cox, R. A., Crowley, J. N., Hampson, R. F., Hynes, R. G., Jenkin, M. E., Rossi, M. J., and Troe, J.: Evaluated kinetic and photochemical data for atmospheric chemistry: Volume III – gas phase reactions of inorganic halogens, Atmos. Chem. Phys., 7, 981–1191, https://doi.org/10.5194/ACP-7-981-2007, 2007.

Bannan, T. J., Booth, A. M., Bacak, A., Muller, J. B. A., Leather, K. E., Le Breton, M., Jones, B., Young, D., Coe, H., Allan, J., Visser, S., Slowik, J. G., Furger, M., Prévôt, A. S. H., Lee, J., Dunmore, R. E., Hopkins, J. R., Hamilton, J. F., Lewis, A. C., Whalley, L. K., Sharp, T., Stone, D., Heard, D. E., Fleming, Z. L., Leigh, R., Shallcross, D. E., and Percival, C. J.: The first UK measurements of nitryl chloride using a chemical ionization mass spectrometer in central London in the summer of 2012, and an investigation of the role of Cl atom oxidation, Journal of Geophysical Research: Atmospheres, 120, 5638–5657, https://doi.org/https://doi.org/10.1002/2014JD022629, 2015.

Behnke, W., George, C., Scheer, V., and Zetzsch, C.: Production and decay of $ClNO_2$ from the reaction of gaseous N_2O_5 with $NaCl$ solution: Bulk and aerosol experiments, J. Geophys. Res., 102D, 3795–3804, https://doi.org/10.1029/96JD03057, 1997.

Bertram, T. H. and Thornton, J. A.: Toward a general parameterization of N_2O_5 reactivity on aqueous particles: the competing effects of particle liquid water, nitrate and chloride, Atmos. Chem. Phys., 9, 8351–8363, https://doi.org/10.5194/ACP-9-8351-2009, 2009.

Brown, S., Stark, H., Ciciora, S., and Ravishankara, A.: In-situ Measurement of Atmospheric NO3 and N2O5 via Cavity Ring-down Spectroscopy, Geophysical Research Letters - GEOPHYS RES LETT, 28, 3227–3230, https://doi.org/10.1029/2001GL013303, 2001.

Brown, S. S., Osthoff, H. D., Stark, H., Dubé, W. P., Ryerson, T. B., Warneke, C., de Gouw, J. A., Wollny, A. G., Parrish, D. D., Fehsenfeld, F. C., and Ravishankara, A.: Aircraft observations of daytime NO3 and N2O5 and their implications for tropospheric chemistry, Journal of Photochemistry and Photobiology A: Chemistry, 176, 270–278, https://doi.org/https://doi.org/10.1016/j.jphotochem.2005.10.004, in Honour of Professor Richard P. Wayne, 2005.

Burkholder, J. B., Sander, S. P., Abbatt, J., Barker, J. R., Huie, R. E., Kolb, C. E., Kurylo, M. J., Orkin, V. L., Wilmouth, D. M., and Wine, P. H.: Chemical Kinetics and Photochemical Data for Use in Atmospheric Studies, Evaluation No. 18, JPL Publication 15-10, Jet Propulsion Laboratory, Pasadena, http://jpldataeval.jpl.nasa.gov, 2015.

Chen, Y., Beig, G., Archer-Nicholls, S., Drysdale, W., Acton, W. J. F., Lowe, D., Nelson, B., Lee, J., Ran, L., Wang, Y., Wu, Z., Sahu, S. K., Sokhi, R. S., Singh, V., Gadi, R., Nicholas Hewitt, C., Nemitz, E., Archibald, A., McFiggans, G., and Wild, O.: Avoiding high ozone pollution in Delhi, India, Faraday Discuss., 226, 502–514, https://doi.org/10.1039/D0FD00079E, 2021.

Choi, M. S., Qiu, X., Zhang, J., Wang, S., Li, X., Sun, Y., Chen, J., and Ying, Q.: Study of Secondary Organic Aerosol Formation from Chlorine Radical-Initiated Oxidation of Volatile Organic Compounds in a Polluted Atmosphere Using a 3D Chemical Transport Model, Environmental Science & Technology, 54, 13 409–13 418, https://doi.org/10.1021/acs.est.0c02958, pMID: 33074656, 2020.

Coombes, R. G., Golding, J. G., and Hadjigeorgiou, P.: Electrophilic aromatic substitution. Part 23. The nitration of phenol and the cresols in aqueous sulphuric acid, J. Chem. Soc. Perkin Trans. 2, pp. 1451–1459, https://doi.org/10.1039/P29790001451, 1979.

Elshorbany, Y. F., Kurtenbach, R., Wiesen, P., Lissi, E., Rubio, M., Villena, G., Gramsch, E., Rickard, A. R., Pilling, M. J., and Kleffmann, J.: Oxidation capacity of the city air of Santiago, Chile, Atmospheric Chemistry and Physics, 9, 2257–2273, https://doi.org/10.5194/acp-9-2257-2009, 2009.

Faxon, C. and Allen, D.: Chlorine chemistry in urban atmospheres: A review, Environmental Chemistry, 10, 221–233, https://doi.org/10.1071/EN13026, 2013.

Frenzel, A., Scheer, V., Sikorski, R., C., G., Behnke, W., and Zetzsch, C.: Heterogeneous interconversion reactions of $BrNO_2$, $ClNO_2$, Br_2, and Cl_2, J. Phys. Chem. A, 102, 1329–1337, https://doi.org/10.1021/JP973044B, 1998.

Fried, A., Henry, B. E., Calvert, J. G., and M., M.: The reaction probability of N_2O_5 with sulfuric acid aerosols at stratospheric temperatures and compositions, J. Geophys. Res., 99D, 3517–3532, https://doi.org/10.1029/93JD01907, 1994.

Geyer, A., Alicke, B., Ackermann, R., Martinez, M., Harder, H., Brune, W., di Carlo, P., Williams, E., Jobson, T., Hall, S., Shetter, R., and Stutz, J.: Direct observations of daytime NO3: Implications for urban boundary layer chemistry, Journal of Geophysical Research: Atmospheres, 108, 4368, https://doi.org/https://doi.org/10.1029/2002JD002967, 2003.

Ghosh, B., Papanastasiou, D. K., Talukdar, R. K., Roberts, J. M., and Burkholder, J. B.: Nitryl Chloride (ClNO2): UV/Vis Absorption Spectrum between 210 and 296 K and O(3P) Quantum Yield at 193 and 248 nm, The Journal of Physical Chemistry A, 116, 5796–5805, https://doi.org/10.1021/jp207389y, pMID: 21936506, 2012.

Golden, D. M.: The Reaction Cl + NO2 → ClONO and ClNO2, The Journal of Physical Chemistry A, 111, 6772–6780, https://doi.org/10.1021/jp069000x, pMID: 17547376, 2007.

Granier, C., Darras, S., van der Gon, H. D., Doubalova, J., Elguindi, N., Galle, B., Gauss, M., Guevara, M., Jalkanen, J.-P., Kuenen, J., Liousse, C., Quack, B., Simpson, D., and Sindelarova, K.: The Copernicus Atmosphere Monitoring Service global and regional emissions (April 2019 version), Copernicus Atmosphere Monitoring Service (CAMS) report, https://doi.org/10.24380/d0bn-kx16, 2019.

Green, M., Yarwood, G., and Niki, H.: FTIR study of the Cl-atom initiated oxidation of methylglyoxal, Int. J. Chem. Kinet., 22, 689–699, https://doi.org/10.1002/KIN.550220705, 1990.

Grigorev, A. E., Makarov, I. E., and Pikaev, A. K.: Formation of Cl_2^- in the bulk solution during the radiolysis of concentrated aqueous solutions of chlorides, High Energy Chem., 21, 99–102, https://kinetics.nist.gov/solution/Detail?id=1987GRI/MAK99-102:2, 1987.

Gunthe, S., Liu, P., Panda, U., S Raj, S., Sharma, A., Darbyshire, E., Reyes Villegas, E., Allan, J., Chen, Y., Wang, X., Song, S., Pohlker, M., Shi, L., Wang, Y., Kommula, S., Liu, T., Ravikrishna, R., Mcfiggans, G., Mickley, L., and Coe, H.: Enhanced aerosol particle growth sustained by high continental chlorine emission in India, Nature Geoscience, 14, https://doi.org/10.1038/s41561-020-00677-x, 2021.

Haskins, J. D., Lee, B. H., Lopez-Hilifiker, F. D., Peng, Q., Jaeglé, L., Reeves, J. M., Schroder, J. C., Campuzano-Jost, P., Fibiger, D., McDuffie, E. E., Jiménez, J. L., Brown, S. S., and Thornton, J. A.: Observational Constraints on the Formation of Cl2 From the Reactive Uptake of ClNO2 on Aerosols in the Polluted Marine Boundary Layer, Journal of Geophysical Research: Atmospheres, 124, 8851–8869, https://doi.org/https://doi.org/10.1029/2019JD030627, 2019.

Haslett, S. L., Bell, D. M., Kumar, V., Slowik, J. G., Wang, D. S., Mishra, S., Rastogi, N., Singh, A., Ganguly, D., Thornton, J., Zheng, F., Li, Y., Nie, W., Liu, Y., Ma, W., Yan, C., Kulmala, M., Daellenbach, K. R., Hadden, D., Baltensperger, U., Prevot, A. S. H., Tripathi, S. N., and Mohr, C.: Nighttime NO emissions strongly suppress chlorine and nitrate radical formation during the winter in Delhi, Atmospheric Chemistry and Physics, 23, 9023–9036, https://doi.org/10.5194/acp-23-9023-2023, 2023.

Heal, M. R., Harrison, M. A. J., and Cape, J. N.: Aqueous-phase nitration of phenol by N_2O_5 and $ClNO_2$, Atmos. Environ., 41, 3515–3520, https://doi.org/10.1016/J.ATMOSENV.2007.02.003, 2007.

Hens, K., Novelli, A., Martinez, M., Auld, J., Axinte, R., Bohn, B., Fischer, H., Keronen, P., Kubistin, D., Nölscher, A. C., Oswald, R., Paasonen, P., Petäjä, T., Regelin, E., Sander, R., Sinha, V., Sipilä, M., Taraborrelli, D., Tatum Ernest, C., Williams, J., Lelieveld, J., and Harder, H.: Observation and modelling of HO$_x$ radicals in a boreal forest, Atmospheric Chemistry and Physics, 14, 8723–8747, https://doi.org/10.5194/acp-14-8723-2014, 2014.

Hersbach, H., Bell, B., Berrisford, P., Hirahara, S., Horányi, A., Muñoz-Sabater, J., Nicolas, J., Peubey, C., Radu, R., Schepers, D., Simmons, A., Soci, C., Abdalla, S., Abellan, X., Balsamo, G., Bechtold, P., Biavati, G., Bidlot, J., Bonavita, M., De Chiara, G., Dahlgren, P., Dee, D., Diamantakis, M., Dragani, R., Flemming, J., Forbes, R., Fuentes, M., Geer, A., Haimberger, L., Healy, S., Hogan, R. J., Hólm, E., Janisková, M., Keeley, S., Laloyaux, P., Lopez, P., Lupu, C., Radnoti, G., de Rosnay, P., Rozum, I., Vamborg, F., Villaume, S., and Thépaut, J.-N.: The ERA5 global reanalysis, Quarterly Journal of the Royal Meteorological Society, 146, 1999–2049, https://doi.org/https://doi.org/10.1002/qj.3803, 2020.

Horowitz, L. W., Fiore, A. M., Milly, G. P., Cohen, R. C., Perring, A., Wooldridge, P. J., Hess, P. G., Emmons, L. K., and Lamarque, J.-F.: Observational constraints on the chemistry of isoprene nitrates over the eastern United States, Journal of Geophysical Research: Atmospheres, 112, https://doi.org/https://doi.org/10.1029/2006JD007747, 2007.

Hossaini, R., Chipperfield, M. P., Saiz-Lopez, A., Fernandez, R., Monks, S., Feng, W., Brauer, P., and von Glasow, R.: A global model of tropospheric chlorine chemistry: Organic versus inorganic sources and impact on methane oxidation, Journal of Geophysical Research: Atmospheres, 121, 14,271–14,297, https://doi.org/https://doi.org/10.1002/2016JD025756, 2016.

Iraci, L. T., Riffel, B. G., Robinson, C. B., Michelsen, R. R., and Stephenson, R. M.: The acid catalyzed nitration of methanol: formation of methyl nitrate via aerosol chemistry, J. Atmos. Chem., 58, 253–266, https://doi.org/10.1007/S10874-007-9091-9, 2007.

Janowski, B., Knauth, H.-D., and Martin, H.: Chlornitrit, ein metastabiles Zwischenprodukt der Reaktion von Dichlormonoxid mit Nitrosylchlorid, Berichte der Bunsengesellschaft für physikalische Chemie, 81, 1262–1270, https://doi.org/https://doi.org/10.1002/bbpc.19770811212, 1977.

Khan, A., Morris, W., Watson, L., Galloway, M., Hamer, P., Shallcross, B., Percival, C., and Shallcross, D.: Estimation of Daytime NO3 Radical Levels in the UK Urban Atmosphere Using the Steady State Approximation Method, Advances in Meteorology, 2015, 9, https://doi.org/10.1155/2015/294069, 2015a.

Khan, M., Cooke, M., Utembe, S., Archibald, A., Derwent, R., Xiao, P., Percival, C., Jenkin, M., Morris, W., and Shallcross, D.: Global modeling of the nitrate radical (NO3) for present and pre-industrial scenarios, Atmospheric Research, 164-165, 347–357, https://doi.org/https://doi.org/10.1016/j.atmosres.2015.06.006, 2015b.

Knipping, E. M., Lakin, M. J., Foster, K. L., Jungwirth, P., Tobias, D. J., Gerber, R. B., Dabdub, D., and Finlayson-Pitts, B. J.: Experiments and simulations of ion-enhanced interfacial chemistry on aqueous NaCl aerosols, Science, 288, 301–306, https://doi.org/10.1126/SCIENCE.288.5464.301, 2000.

Kroflič, A., Grilc, M., and Grgić, I.: Unraveling Pathways of Guaiacol Nitration in Atmospheric Waters: Nitrite, A Source of Reactive Nitronium Ion in the Atmosphere, Environmental Science & Technology, 49, 9150–9158, https://doi.org/10.1021/acs.est.5b01811, pMID: 26162010, 2015.

Landgraf, J. and Crutzen, P. J.: An efficient method for online calculations of photolysis and heating rates, J. Atmos. Sci., 55, 863–878, https://doi.org/10.1175/1520-0469(1998)055<0863:AEMFOC>2.0.CO;2, 1998.

Lanz, V. A., Prévôt, A. S. H., Alfarra, M. R., Weimer, S., Mohr, C., DeCarlo, P. F., Gianini, M. F. D., Hueglin, C., Schneider, J., Favez, O., D'Anna, B., George, C., and Baltensperger, U.: Characterization of aerosol chemical composition with aerosol mass spectrometry in Central Europe: an overview, Atmospheric Chemistry and Physics, 10, 10 453–10 471, https://doi.org/10.5194/acp-10-10453-2010, 2010.

Lawler, M. J., Sander, R., Carpenter, L. J., Lee, J. D., von Glasow, R., Sommariva, R., and Saltzman, E. S.: HOCl and Cl$_2$ observations in marine air, Atmospheric Chemistry and Physics, 11, 7617–7628, https://doi.org/10.5194/acp-11-7617-2011, 2011.

Liao, J., Huey, L., Liu, Z., Tanner, D., Cantrell, C., Orlando, J., Flocke, F., Shepson, P., Weinheimer, A., Hall, S., Ullmann, K., Beine, H., Wang, Y., Ingall, E., Stephens, C., Hornbrook, R., Apel, E., Riemer, D., Fried, A., and Nowak, J.: High levels of molecular chlorine in the Arctic atmosphere, Nature Geoscience, 7, https://doi.org/10.1038/ngeo2046, 2014.

Liu, X., Qu, H., Huey, L. G., Wang, Y., Sjostedt, S., Zeng, L., Lu, K., Wu, Y., Hu, M., Shao, M., Zhu, T., and Zhang, Y.: High Levels of Daytime Molecular Chlorine and Nitryl Chloride at a Rural Site on the North China Plain, Environmental Science & Technology, 51, 9588–9595, https://doi.org/10.1021/acs.est.7b03039, pMID: 28806070, 2017.

Lobert, J. M., Keene, W. C., Logan, J. A., and Yevich, R.: Global chlorine emissions from biomass burning: Reactive Chlorine Emissions Inventory, Journal of Geophysical Research: Atmospheres, 104, 8373–8389, https://doi.org/https://doi.org/10.1029/1998JD100077, 1999.

Müller, B. and Heal, M. R.: The Henry's law coefficient of 2-nitrophenol over the temperature range 278-303 K, Chemosphere, 45, 309–314, https://doi.org/10.1016/S0045-6535(00)00592-0, 2001.

Nakoudi, K., Giannakaki, E., Dandou, A., Tombrou, M., and Komppula, M.: Planetary Boundary Layer variability over New Delhi, India, during EUCAARI project, Atmospheric Measurement Techniques Discussions, pp. 1–33, https://doi.org/10.5194/amt-2018-342, 2018.

Nelson, B. S., Stewart, G. J., Drysdale, W. S., Newland, M. J., Vaughan, A. R., Dunmore, R. E., Edwards, P. M., Lewis, A. C., Hamilton, J. F., Acton, W. J., Hewitt, C. N., Crilley, L. R., Alam, M. S., Şahin, U. A., Beddows, D. C. S., Bloss, W. J., Slater, E., Whalley, L. K., Heard, D. E., Cash, J. M., Langford, B., Nemitz, E., Sommariva, R., Cox, S., Shivani, Gadi, R., Gurjar, B. R., Hopkins, J. R., Rickard, A. R., and Lee, J. D.: In situ ozone production is highly sensitive to volatile organic compounds in Delhi, India, Atmospheric Chemistry and Physics, 21, 13 609–13 630, https://doi.org/10.5194/acp-21-13609-2021, 2021.

Nelson, B. S., Bryant, D. J., Alam, M. S., Sommariva, R., Bloss, W. J., Newland, M. J., Drysdale, W. S., Vaughan, A. R., Acton, W. J. F., Hewitt, C. N., Crilley, L. R., Swift, S. J., Edwards, P. M., Lewis, A. C., Langford, B., Nemitz, E., Shivani, Gadi, R., Gurjar, B. R., Heard, D. E., Whalley, L. K., Sahin, U. A., Beddows, D. C. S., Hopkins, J. R., Lee, J. D., Rickard, A. R., and Hamilton, J. F.: Extreme Concentrations of Nitric Oxide Control Daytime Oxidation and Quench Nocturnal Oxidation Chemistry in Delhi during Highly Polluted Episodes, Environmental Science & Technology Letters, 10, 520–527, https://doi.org/10.1021/acs.estlett.3c00171, 2023.

Niki, H., Maker, P., Savage, C., and Breitenbach, L.: Fourier transform IR spectroscopic observation of chlorine nitrite, ciono, formed via Cl + NO2 (+M) → ClONO(+M), Chemical Physics Letters, 59, 78–79, https://doi.org/https://doi.org/10.1016/0009-2614(78)85618-8, 1978.

Niki, H., Maker, P. D., Savage, C. M., and Breitenbach, L. P.: An FTIR study of the Cl-atom-initiated reaction of glyoxal, Int. J. Chem. Kinet., 17, 547–558, https://doi.org/10.1002/KIN.550170507, 1985.

Niki, H., Maker, P. D., Savage, C. M., and Hurley, M. D.: Fourier transform infrared study of the kinetics and mechanisms for the Cl-atom- and HO-radical-initiated oxidation of glycolaldehyde, J. Phys. Chem., 91, 2174–2178, https://doi.org/10.1021/J100292A038, 1987.

Nölscher, A., Butler, T., Auld, J., Veres, P., Muñoz, A., Taraborrelli, D., Vereecken, L., Lelieveld, J., and Williams, J.: Using total OH reactivity to assess isoprene photooxidation via measurement and model, Atmospheric Environment, 89, 453–463, https://doi.org/https://doi.org/10.1016/j.atmosenv.2014.02.024, 2014.

Osthoff, H. D., Roberts, J. M., Ravishankara, A. R., Williams, E. J., Lerner, B. M., Sommariva, R., Bates, T. S., Coffman, D., Quinn, P. K., Dibb, J. E., Stark, H., Burkholder, J. B., Talukdar, R. K., Meagher, J., Fehsenfeld, F. C., and Brown, S. S.: High levels of nitryl chloride in the polluted subtropical marine boundary layer, Nature Geosci., 1, 324–328, https://doi.org/10.1038/NGEO177, 2008.

Pawar, P. V., Ghude, S. D., Govardhan, G., Acharja, P., Kulkarni, R., Kumar, R., Sinha, B., Sinha, V., Jena, C., Gunwani, P., Adhya, T. K., Nemitz, E., and Sutton, M. A.: Chloride (HCl/Cl^-) dominates inorganic aerosol formation from ammonia in the Indo-Gangetic Plain during winter: modeling and comparison with observations, Atmospheric Chemistry and Physics, 23, 41–59, https://doi.org/10.5194/acp-23-41-2023, 2023.

Pozzer, A., Reifenberg, S. F., Kumar, V., Franco, B., Kohl, M., Taraborrelli, D., Gromov, S., Ehrhart, S., Jöckel, P., Sander, R., Fall, V., Rosanka, S., Karydis, V., Akritidis, D., Emmerichs, T., Crippa, M., Guizzardi, D., Kaiser, J. W., Clarisse, L., Kiendler-Scharr, A., Tost, H., and Tsimpidi, A.: Simulation of organics in the atmosphere: evaluation of EMACv2.54 with the Mainz Organic Mechanism (MOM) coupled to the ORACLE (v1.0) submodel, Geoscientific Model Development, 15, 2673–2710, https://doi.org/10.5194/gmd-15-2673-2022, 2022.

Qiu, X., Ying, Q., Wang, S., Duan, L., Wang, Y., Lu, K., Wang, P., Xing, J., Zheng, M., Zhao, M., Zheng, H., Zhang, Y., and Hao, J.: Significant impact of heterogeneous reactions of reactive chlorine species on summertime atmospheric ozone and free-radical formation in north China, Sci. Total Environ., 693, 133 580, https://doi.org/10.1016/J.SCITOTENV.2019.133580, 2019a.

Qiu, X., Ying, Q., Wang, S., Duan, L., Zhao, J., Xing, J., Ding, D., Sun, Y., Liu, B., Shi, A., Yan, X., Xu, Q., and Hao, J.: Modeling the impact of heterogeneous reactions of chlorine on summertime nitrate formation in Beijing, China, Atmospheric Chemistry and Physics, 19, 6737–6747, https://doi.org/10.5194/acp-19-6737-2019, 2019b.

Ravishankara, A. R.: Are chlorine atoms significant tropospheric free radicals?, Proceedings of the National Academy of Sciences, 106, 13 639–13 640, https://doi.org/10.1073/pnas.0907089106, 2009.

Rickard, A.: Master Chemical Mechanism, MCM v3.3.1, http://mcm.york.ac.uk, 2009.

Riedel, T. P., Wolfe, G. M., Danas, K. T., Gilman, J. B., Kuster, W. C., Bon, D. M., Vlasenko, A., Li, S.-M., Williams, E. J., Lerner, B. M., Veres, P. R., Roberts, J. M., Holloway, J. S., Lefer, B., Brown, S. S., and Thornton, J. A.: An MCM modeling study of nitryl chloride ($ClNO_2$) impacts on oxidation, ozone production and nitrogen oxide partitioning in polluted continental outflow, Atmospheric Chemistry and Physics, 14, 3789–3800, https://doi.org/10.5194/acp-14-3789-2014, 2014.

Roberts, J. M., Osthoff, H. D., Brown, S. S., and Ravishankara, A. R.: N_2O_5 oxidizes chloride to Cl_2 in acidic atmospheric aerosol, Science, 321, 1059, https://doi.org/10.1126/SCIENCE.1158777, 2008.

Roberts, J. M., Osthoff, H. D., Brown, S. S., Ravishankara, A. R., Coffman, D., Quinn, P., and Bates, T.: Laboratory studies of products of N2O5 uptake on Cl-containing substrates, Geophysical Research Letters, 36, https://doi.org/https://doi.org/10.1029/2009GL040448, 2009.

Rosanka, S., Sander, R., Wahner, A., and Taraborrelli, D.: Oxidation of low-molecular-weight organic compounds in cloud droplets: development of the Jülich Aqueous-phase Mechanism of Organic Chemistry (JAMOC) in CAABA/MECCA (version 4.5.0), Geoscientific Model Development, 14, 4103–4115, https://doi.org/10.5194/gmd-14-4103-2021, 2021.

Ryder, O. S., Campbell, N. R., Shaloski, M., Al-Mashat, H., Nathanson, G. M., and Bertram, T. H.: Role of organics in regulating $ClNO_2$ production at the air-sea interface, J. Phys. Chem. A, 119, 8519–8526, https://doi.org/10.1021/JP5129673, 2015.

Saiz-Lopez, A. and von Glasow, R.: Reactive halogen chemistry in the troposphere, Chem. Soc. Rev., 41, 6448–6472, https://doi.org/10.1039/C2CS35208G, 2012.

Sander, R.: Compilation of Henry's law constants (version 4.0) for water as solvent, Atmos. Chem. Phys., 15, 4399–4981, https://doi.org/10.5194/ACP-15-4399-2015, 2015.

Sander, R., Jöckel, P., Kirner, O., Kunert, A. T., Landgraf, J., and Pozzer, A.: The photolysis module JVAL-14, compatible with the MESSy standard, and the JVal PreProcessor (JVPP), Geoscientific Model Development, 7, 2653–2662, https://doi.org/10.5194/gmd-7-2653-2014, 2014.

Sander, R., Baumgaertner, A., Cabrera-Perez, D., Frank, F., Gromov, S., Grooß, J.-U., Harder, H., Huijnen, V., Jöckel, P., Karydis, V. A., Niemeyer, K. E., Pozzer, A., Riede, H., Schultz, M. G., Taraborrelli, D., and Tauer, S.: The community atmospheric chemistry box model CAABA/MECCA-4.0, Geoscientific Model Development, 12, 1365–1385, https://doi.org/10.5194/gmd-12-1365-2019, 2019.

575 Sandu, A. and Sander, R.: Technical note: Simulating chemical systems in Fortran90 and Matlab with the Kinetic PreProcessor KPP-2.1, Atmos. Chem. Phys., 6, 187–195, https://doi.org/10.5194/ACP-6-187-2006, 2006.

Sapoli, M., De Santis, A., Marziano, N. C., Pinna, F., and Zingales, A.: Equilibria of nitric acid in sulfuric and perchloric acid at 25.degree.C by Raman and UV spectroscopy, The Journal of Physical Chemistry, 89, 2864–2869, https://doi.org/10.1021/j100259a032, 1985.

Sarwar, G., Simon, H., Xing, J., and Mathur, R.: Importance of tropospheric ClNO2 chemistry across the Northern Hemisphere, Geophysical
580 Research Letters, 41, 4050–4058, https://doi.org/https://doi.org/10.1002/2014GL059962, 2014.

Seinfeld, J. H. and Pandis, S. N.: Atmospheric Chemistry and Physics, John Wiley & Sons, Inc., 2016.

Sharma, G., Sinha, B., Pallavi, Hakkim, H., Chandra, B. P., Kumar, A., and Sinha, V.: Gridded Emissions of CO, NOx, SO2, CO2, NH3, HCl, CH4, PM2.5, PM10, BC, and NMVOC from Open Municipal Waste Burning in India, Environmental Science & Technology, 53, 4765–4774, https://doi.org/10.1021/acs.est.8b07076, 2019.

585 Shi, J. and Bernhard, M. J.: Kinetic studies of Cl-atom reactions with selected aromatic compounds using the photochemical reactor-FTIR spectroscopy technique, Int. J. Chem. Kinet., 29, 349–358, https://doi.org/10.1002/(SICI)1097-4601(1997)29:5<349::AID-KIN5>3.0.CO;2-U, 1997.

Sindelarova, K., Granier, C., Bouarar, I., Guenther, A., Tilmes, S., Stavrakou, T., Müller, J.-F., Kuhn, U., Stefani, P., and Knorr, W.: Global data set of biogenic VOC emissions calculated by the MEGAN model over the last 30 years, Atmospheric Chemistry and Physics, 14,
590 9317–9341, https://doi.org/10.5194/acp-14-9317-2014, 2014.

Sokolov, O., Hurley, M. D., Ball, J. C., Wallington, T. J., Nelsen, W., Barnes, I., and Becker, K. H.: Kinetics of the reactions of chlorine atoms with CH_3ONO and CH_3ONO_2, Int. J. Chem. Kinet., 31, 357–359, https://doi.org/10.1002/(SICI)1097-4601(1999)31:5<357::AID-KIN5>3.0.CO;2-6, 1999.

Sommariva, R., Hollis, L. D. J., Sherwen, T., Baker, A. R., Ball, S. M., Bandy, B. J., Bell, T. G., Chowdhury, M. N., Cordell, R. L., Evans,
595 M. J., Lee, J. D., Reed, C., Reeves, C. E., Roberts, J. M., Yang, M., and Monks, P. S.: Seasonal and geographical variability of nitryl chloride and its precursors in Northern Europe, Atmospheric Science Letters, 19, e844, https://doi.org/https://doi.org/10.1002/asl.844, 2018.

Sommariva, R., Crilley, L. R., Ball, S. M., Cordell, R. L., Hollis, L. D., Bloss, W. J., and Monks, P. S.: Enhanced wintertime oxidation of VOCs via sustained radical sources in the urban atmosphere, Environmental Pollution, 274, 116 563,
600 https://doi.org/https://doi.org/10.1016/j.envpol.2021.116563, 2021.

Soni, M., Sander, R., Taraborrelli, D., and Ojha, N.: Model outputs associated with "Comprehensive multiphase chlorine chemistry in the box model CAABA/MECCA: Implications to atmospheric oxidative capacity" [Data set], Zenodo, https://doi.org/10.5281/zenodo.8332131, 2023.

Staudt, S., Gord, J. R., Karimova, N. V., McDuffie, E. E., Brown, S. S., Gerber, R. B., Nathanson, G. M., and Bertram,
605 T. H.: Sulfate and carboxylate suppress the formation of $ClNO_2$ at atmospheric interfaces, Earth Space Chem., 3, 1987–1997, https://doi.org/10.1021/ACSEARTHSPACECHEM.9B00177, 2019.

Taraborrelli, D., Lawrence, M. G., Crowley, J. N., Dillon, T. J., Gromov, S., Groß, C. B. M., Vereecken, L., and Lelieveld, J.: Hydroxyl radical buffered by isoprene oxidation over tropical forests, Nature Geosci., 5, 190–193, https://doi.org/10.1038/NGEO1405, 2012.

Taraborrelli, D., Cabrera-Perez, D., Bacer, S., Gromov, S., Lelieveld, J., Sander, R., and Pozzer, A.: Influence of aromatics on tropospheric
610 gas-phase composition, Atmospheric Chemistry and Physics, 21, 2615–2636, https://doi.org/10.5194/acp-21-2615-2021, 2021.

Tham, Y. J., Wang, Z., Li, Q., Yun, H., Wang, W., Wang, X., Xue, L., Lu, K., Ma, N., Bohn, B., Li, X., Kecorius, S., Größ, J., Shao, M., Wiedensohler, A., Zhang, Y., and Wang, T.: Significant concentrations of nitryl chloride sustained in the morning: investigations of the

causes and impacts on ozone production in a polluted region of northern China, Atmospheric Chemistry and Physics, 16, 14 959–14 977, https://doi.org/10.5194/acp-16-14959-2016, 2016.

615 Thiault, G., Mellouki, A., and Bras, G. L.: Kinetics of gas phase reactions of OH and Cl with aromatic aldehydes, Phys. Chem. Chem. Phys., 4, 2194–2199, https://doi.org/10.1039/b200609j, 2002.

Thornton, J., Kercher, J., Riedel, T., Wagner, N., Cozic, J., Holloway, J., Dubé, W., Wolfe, G., Quinn, P., Middlebrook, A., Alexander, B., and Brown, S.: A large atomic chlorine source inferred from mid-continental reactive nitrogen chemistry, Nature, 464, 271–4, https://doi.org/10.1038/nature08905, 2010.

620 Tripathi, N., Sahu, L. K., Wang, L., Vats, P., Soni, M., Kumar, P., Satish, R. V., Bhattu, D., Sahu, R., Patel, K., Rai, P., Kumar, V., Rastogi, N., Ojha, N., Tiwari, S., Ganguly, D., Slowik, J., Prévôt, A. S. H., and Tripathi, S. N.: Characteristics of VOC Composition at Urban and Suburban Sites of New Delhi, India in Winter, Journal of Geophysical Research: Atmospheres, 127, e2021JD035 342, https://doi.org/https://doi.org/10.1029/2021JD035342, e2021JD035342 2021JD035342, 2022.

von Glasow, R. and Crutzen, P.: Tropospheric Halogen Chemistry, in: Treatise on Geochemistry, edited by Holland, H. D. and Turekian,
625 K. K., Pergamon, Oxford, 2007.

Wang, L., Arey, J., and Atkinson, R.: Reactions of chlorine atoms with a series of aromatic hydrocarbons, Environ. Sci. Technol., 39, 5302–5310, https://doi.org/10.1021/ES0479437, 2005.

Wang, T., Tham, Y. J., Xue, L., Li, Q., Zha, Q., Wang, Z., Poon, S. C. N., Dubé, W. P., Blake, D. R., Louie, P. K. K., Luk, C. W. Y., Tsui, W., and Brown, S. S.: Observations of nitryl chloride and modeling its source and effect on ozone in the planetary boundary layer of southern
630 China, Journal of Geophysical Research: Atmospheres, 121, 2476–2489, https://doi.org/https://doi.org/10.1002/2015JD024556, 2016.

Wennberg, P. O., Bates, K. H., Crounse, J. D., Dodson, L. G., McVay, R. C., Mertens, L. A., Nguyen, T. B., Praske, E., Schwantes, R. H., Smarte, M. D., St Clair, J. M., Teng, A. P., Zhang, X., and Seinfeld, J. H.: Gas-Phase Reactions of Isoprene and Its Major Oxidation Products, Chemical Reviews, 118, 3337–3390, https://doi.org/10.1021/acs.chemrev.7b00439, pMID: 29522327, 2018.

Xue, L. K., Saunders, S. M., Wang, T., Gao, R., Wang, X. F., Zhang, Q. Z., and Wang, W. X.: Development of a chlorine chemistry module
635 for the Master Chemical Mechanism, Geoscientific Model Development, 8, 3151–3162, https://doi.org/10.5194/gmd-8-3151-2015, 2015.

Young, C. J., Washenfelder, R. A., Roberts, J. M., Mielke, L. H., Osthoff, H. D., Tsai, C., Pikelnaya, O., Stutz, J., Veres, P. R., Cochran, A. K., VandenBoer, T. C., Flynn, J., Grossberg, N., Haman, C. L., Lefer, B., Stark, H., Graus, M., de Gouw, J., Gilman, J. B., Kuster, W. C., and Brown, S. S.: Vertically Resolved Measurements of Nighttime Radical Reservoirs in Los Angeles and Their Contribution to the Urban Radical Budget, Environmental Science & Technology, 46, 10 965–10 973, https://doi.org/10.1021/es302206a, pMID: 23013316, 2012.

640 Zhang, B., Shen, H., Yun, X., Zhong, Q., Henderson, B. H., Wang, X., Shi, L., Gunthe, S. S., Huey, L. G., Tao, S., Russell, A. G., and Liu, P.: Global Emissions of Hydrogen Chloride and Particulate Chloride from Continental Sources, Environmental Science & Technology, 56, 3894–3904, https://doi.org/10.1021/acs.est.1c05634, pMID: 35319880, 2022.

Zhang, L., Li, Q., Wang, T., Ahmadov, R., Zhang, Q., Li, M., and Lv, M.: Combined impacts of nitrous acid and nitryl chloride on lower-tropospheric ozone: new module development in WRF-Chem and application to China, Atmospheric Chemistry and Physics, 17, 9733–
645 9750, https://doi.org/10.5194/acp-17-9733-2017, 2017.

Zhang, Q., Jimenez, J. L., Canagaratna, M. R., Allan, J. D., Coe, H., Ulbrich, I., Alfarra, M. R., Takami, A., Middlebrook, A. M., Sun, Y. L., Dzepina, K., Dunlea, E., Docherty, K., DeCarlo, P. F., Salcedo, D., Onasch, T., Jayne, J. T., Miyoshi, T., Shimono, A., Hatakeyama, S., Takegawa, N., Kondo, Y., Schneider, J., Drewnick, F., Borrmann, S., Weimer, S., Demerjian, K., Williams, P., Bower, K., Bahreini, R., Cottrell, L., Griffin, R. J., Rautiainen, J., Sun, J. Y., Zhang, Y. M., and Worsnop, D. R.: Ubiquity and dominance of oxygenated species

650   in organic aerosols in anthropogenically-influenced Northern Hemisphere midlatitudes, Geophysical Research Letters, 34, L13 801, https://doi.org/https://doi.org/10.1029/2007GL029979, 2007.